Nano Research

ISSN 1998-0124 CN 11-5974/O4
https://doi.org/10.1007/s12274-019-2300-4

Review Article

Graphene oxide-based hydrogels as a nanocarrier for anticancer drug delivery

Abdullah A.Ghawanmeh[1], Gomaa A. M. Ali[1,2], H. Algarni[3,4], Shaheen M. Sarkar[5], and Kwok Feng Chong[1] (✉)

[1] *Faculty of Industrial Sciences & Technology, Universiti Malaysia Pahang, Gambang, 26300 Kuantan, Malaysia*
[2] *Chemistry Department, Faculty of Science, Al–Azhar University, Assiut, 71524, Egypt*
[3] *Department of Physics, Faculty of Sciences, King Khalid University, Abha 61413, P. O. Box 9004, Saudi Arabia*
[4] *Research Center for Advanced Materials Science (RCAMS), King Khalid University, Abha 61413, P. O. Box 9004, Saudi Arabia*
[5] *Bernal Institute, Department of Chemical Sciences, University of Limerick, Castletroy, V94 Limerick, Ireland*

Received: 22 October 2018 / **Revised:** 12 January 2019 / **Accepted:** 15 January 2019

ABSTRACT

Graphene oxide (GO) possesses excellent mechanical strength, biocompatibility, colloidal stability, large surface area and high adsorption capability. It has driven to cancer nanotechnology to defeat cancer therapy obstacles, via integration into three-dimensional (3D) hydrogel network with biocompatible polymers as nanocomposites carrier, and controllable release of anticancer drugs. Specifically, the surface of GO affords π-π stacking and hydrophilic interactions with anticancer drugs. Additionally, modification of GO with various polymers such as natural and synthetic polymers enhances its biodegradability, drug loading, and target delivery. In this review, GO based hydrogels research accomplishments are reviewed on the aspects of crosslinking strategies, preparation methods, the model drug, polymer conjugation and modification with targeting ligands. Moreover, swelling kinetics, drug release profile and biological activity *in vivo* and *in vitro* are discussed. The biocompatibility of GO based hydrogels is also discussed from the perspective of its nano-bio interfaces. Apart from that, the clinical potential of GO based hydrogels and its major challenges are addressed in detail. Finally, this review concludes with a summary and invigorating future perspectives of GO based hydrogels for anticancer drug delivery. It is anticipated that this review can stimulate a new research gateway to facilitate the development of anticancer drug delivery by harnessing the unique properties of GO based hydrogels, such as large surface area, chemical purity, high loading capacity of drug, chemical stability, and the nature of lipophilic for cell membrane penetration.

KEYWORDS

graphene oxide, cancer nanotechnology, hydrogel, nanocarrier, drug delivery

1 Introduction

Today, cancer is the most dangerous disease that leads to death. It can be defined as a complex multifunctional cell disease that originates from genetic and molecular abnormalities [1]. GLOBOCAN statistics showed in 2012, about 14.1 million new cancer cases and 8.2 million death cases occurred [2]. Several methods have been used for the cancer treatment including surgery, radiation therapy and chemotherapy. However, limitations to those methods were documented, with regards to the side effects due to higher drug toxicity and the method efficiency [3]. Cancer nanotechnology is a new research field to develop a tool that overcomes barriers in cancer therapies, by applying nanoparticles as drug delivery agents [4]. The main reason behind exploring nanoparticles as drug delivery agent is attributed to their small sizes below 100 nm, which can easily gain access to a tumor cell and get more time to retain inside the tumor [5, 6]. In addition, at molecular level, the mesoscopic size property supports the unique interaction with biological systems. Moreover, nanoparticles are very important to drug encapsulation and biocompatibility, owing to their material composition to provide self-assembling property and maintain the specificity and stability [4]. Different kinds of materials were used for the preparation of nanoparticles-based therapeutic systems, such as carbon, ceramic, polymers, lipids and metals [7, 8]. Moreover, therapeutic systems can be synthesized in different shapes including spherical, tubular or branched structure [8]. Therefore, the type of nanoparticles used for drug delivery system undergoes various development such as polymer microspheres, polymer-drug conjugates, micelles, and various ligand-targeted products [9, 10].

Utilization of nanotechnology as drug delivery system might encounter several challenges, including stability, site-specific delivery and programmed drug release [11]. Accordingly, anticancer drug administration must overcome series of obstructions that lead to side effects on the normal cells other than target cells throughout blood circulation. Moreover, nanocarriers during delivering drugs into targeted cancer cells prefer tumor aggregation via the enhanced permeability and retention effect and affinity to the uptake of receptor-specific cellular [12]. To regulate the anticancer drug release and deliver it to the targeted site, the researchers had studied the physicochemical properties and micro-environmental features of tumor tissues, which are unique, compared to normal tissues, such as gradients of abnormal temperature, overexpressed proteins and enzymes as well as weak acidity [13–15]. Specifically, at the intracellular level, there are remarkable differences in the micro-environment between the tumor cells and the normal cells, such as the high glutathione level or cysteine in the endolysosomes and cytoplasm,

Address correspondence to ckfeng@ump.edu.my

reductive micro-environments, the pH (5.0–5.5) inside lysosomes and endosomes [16, 17].

In the last two decades, attention went toward hydrogel nanoparticles as one of the most promising techniques in drug delivery systems. It is a hybrid system combing hydrophilicity and the high water content characteristics (hydrogel), with small size nanoparticles [16–21]. The advantages are mainly focusing on safety improvement and drugs efficiency. Additionally, bioavailability and stability of the drug against degradation (chemical or enzymatic) [20–22] are widely studied. In general, the hydrogel is defined as a crosslinked three-dimensional (3D) network of hydrophilic polymeric chains, which is capable to hold a lot of water, as a result of their hydrophilic structures containing functional groups such as –OH, COOH, CONH, $CONH_2$, and $–SO_3H$ [18, 23–25]. The presence of these groups and the polymer composition, enable it to hydrate to different degrees. Although, the hydrogel has the swelling behavior other than being dissolved in aqueous media, where the effect of crosslinker (physically or chemically) presents in their structure, by providing covalent bonds, hydrogen bonding, or van der Waals interactions into the polymeric network [26].

The applications of hydrogels in different biomedical fields can be attributed to their properties such as simple preparation, unique biocompatibility, desirable physical characteristics, and constituents range. Although, they possess the living tissue properties, by controlling the protein and drug delivery, and barrier serving between material surfaces and tissues. As a result, the mechanical, swelling and biocompatible properties of hydrogels must be evaluated before being applied [27].

Graphene is two-dimensional (2D) mono-layer of an atomic thick sheet of sp^2 hybridized honeycomb carbon atoms. Graphene is an attractive candidate for various disciplines including chemistry and physics [28]. Graphene and its derivatives have catalysed the growth in electronics, computers and solar cells technology [29, 30]. Graphene has properties of water-dispersible, biocompatible, and non-toxic, which lead to its proposal for biomedical application such as anticancer therapy, biomedical imaging, and drug delivery. It is the basic building block for all carbon nanomaterials, like fullerene, carbon nanotubes and graphite (3D) [31]. Since its first isolation in 2004, graphene has become the most interested topics in the fields of materials science, physics and chemistry [32]. Graphene structure has reactive sites for surface reaction and free π electrons, which provide potential prospects for the development of different functionalities [33]. Moreover, the planar system of graphene demonstrates distinctive physicochemical properties, predominantly related to high electronic and thermal conductivity [34]. Graphene oxide (GO), a chemically modified graphene in highly oxidized form is water-soluble, which consists of epoxide and hydroxyl (OH) functional groups on the two sides of a single thick layer of graphene, and at the edges carboxylic (COOH) groups (Fig. 1) [35, 36].

GO contains unmodified areas, which have free π electrons and those areas are hydrophobic that enable drug loading by van der Waals forces [28, 37]. The polarity of epoxide, hydroxyl and carboxylic acid groups make hydrogen bonding and other reactions occur on the surface of GO [38].

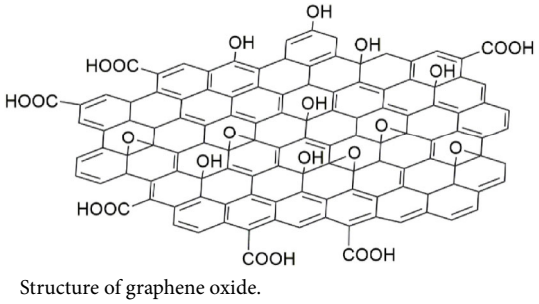

Figure 1 Structure of graphene oxide.

Additionally, many graphene derivatives have been investigated for biomedical applications (Fig. 2) [39]. Attempt to optimize the properties of GO in biomedical application had been started in 2008, where Liu's group used PEGylated graphene labeled with a radionuclide to study the pharmacokinetics and biodistribution of graphene, in which they carried out several examinations of these functionalized materials on mice [40]. Recently, a complex of polyethyleneimine (PEI), polyethylene glycol (PEG) and folic acid (FA) covalently functionalized on GO was synthesized as a nanocarrier system for targeting hepatocellular carcinoma therapy. The electrostatic adsorption method was employed in that work to load si-Stat3 antibody (GO-PEI-PEG-FA/si-Stat3) [41]. In biomedical applications, the physicochemical properties of GO, such as reliable aqueous dispersibility and colloidal stability, render it as versatile and feasible material for drug delivery and therapeutic applications [39].

In this review, an overview of productions of GO from graphite, polymers/GO hydrogel as anticancer delivery agents research will be discussed. In addition, unmodified GO as an anticancer drug carrier, the type of crosslinkers used for the preparation of hydrogel and anticancer model drug used for controlled release system besides *in vitro* and *in vivo* studies will be highlighted.

2 Hydrogels

As mentioned, hydrogels are water-soluble 3D crosslinked networks that can be shaped into a thin film, sphere, cylinder and irregular solid. The drug release kinetics can be affected by the hydrogel geometry [42]. Furthermore, the hydrogel is capable of swelling in water without dissolving, which can be attributed to the hydrophilic functional groups linked to the polymer backbone. Its resistance in water-dissolution is originated from the crosslinking in polymeric networks [43]. The pore size in hydrogel network plays an important role in water swelling, and it can be easily controlled by the crosslinker density in the hydrogel matrix. The higher crosslinker density can improve the mechanical properties, but at the cost of lower swelling ratio. Consequently, the optimization is required to improve the physical properties of hydrogel [44, 45].

2.1 History of hydrogel

The hydrogel term appeared in the year 1894, and it was described as a colloidal gel made with inorganic salts [46]. The current term of hydrogel used for biological application was originated in 1960 when Wichterle and Lim developed a poly(2-hydroxyethyl methacrylate) (pHEMA) hydrogel with high water swelling ratio [47]. Afterward, the number of hydrogel research has increased in the 70's decade

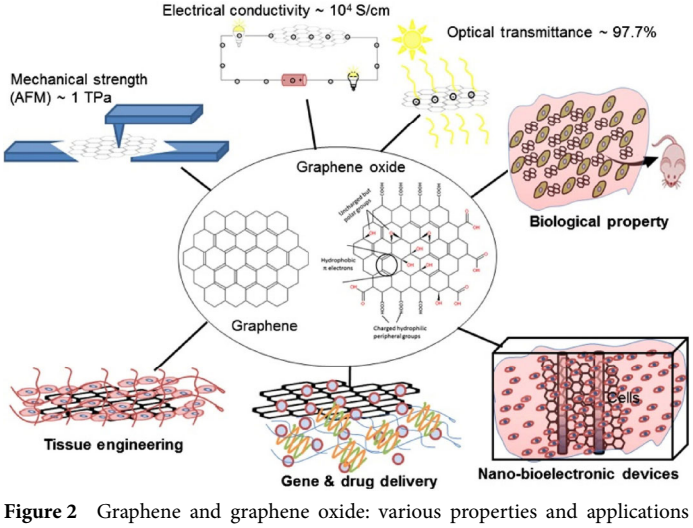

Figure 2 Graphene and graphene oxide: various properties and applications (Adapted with permission from Ref. [28], © Elsevier Ltd. 2014).

[46]. During the period of 2000–2010, the total number of hydrogel publications under different topics, including drug delivery, nanotechnology, and smart hydrogels, had grown up to reach 5,000 publications [46].

Buwalda et al. categorized the history of hydrogels into three generations [48]. In the first generation, (1894–1969), it covers the chemical synthesis methods of hydrogels starting from monomers or polymer using different crosslinker. Additionally, the physicochemical properties, like hydrophilicity of monomers or polymer, hydrogel swelling, and crosslinker density were studied. In the second generation, (1970–1990), it covers the hydrogels with stimuli response such as pH, temperature, and biomolecules concentration. These stimuli could trigger to induce specific action, like drug release. Finally, in the third generation (1991–present), it covers the interaction (crosslink) methods for hydrogel preparation from stereo complexed materials, such as PEG-PLLA, Cyclodextrins-polypseudororaxane.

2.2 Classification of hydrogels

Hydrogels are classified on different bases such as sources, polymer composition, configuration, type of crosslinking, physical appearance, and network electrical charge. Source-based hydrogel classification could be the natural origin or synthetic one (Fig. 3) [49], whereas the polymer composition classification of the hydrogel can be homopolymeric, copolymeric and multipolymer networks. Homopolymeric hydrogels made from single monomer species and copolymeric hydrogels contain two or more different monomers, and commonly one of them possesses hydrophilic properties. Additionally, the chain arrangement in the polymer backbone could be on the block, alternating or random configurations. Multipolymer networks are an important group of hydrogels, and it can be categorized as Semi-Interpenetrating (Semi-IPNs) and Interpenetrating Networks (IPNs). In IPNs system, all polymers are completely crosslinked (chemical bonds). Nonetheless, in Semi-IPNs system, one polymer is crosslinked while other non-crosslinked and trapped within the first cross-linked polymer hydrogel to form partially penetrating networks [43, 49, 50].

On the bases of configuration [43], hydrogels can be classified into crystalline, semicrystalline and amorphous (non-crystalline), depending on the chemical composition and their physical structure. In semicrystalline, the composition consists of the two phases of amorphous and crystalline.

In the physical appearance classifications of the hydrogel, the technique used for hydrogel synthesis determine their appearance as microsphere, matrix or film [43]. The type of crosslinking in hydrogel classification could be physical or chemical. In physical crosslinking, the junction is made by the entanglement of the polymer chain or secondary forces like hydrophobic interactions, ionic interactions, or hydrogen bonding. On the other hand, strong chemical bonding, commonly as a covalent bond can be found in chemical cross-linking [43, 49, 51].

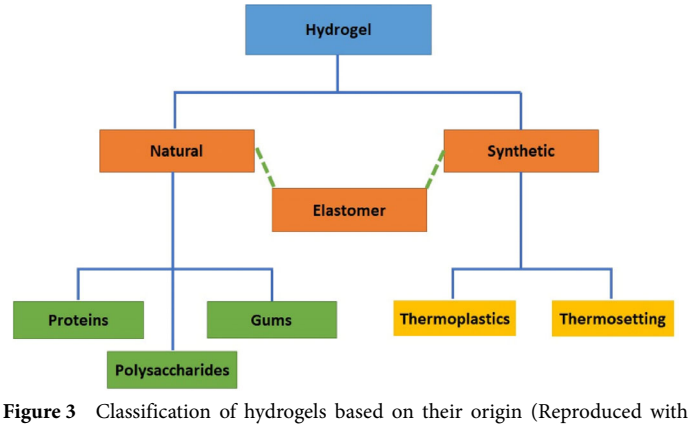

Figure 3 Classification of hydrogels based on their origin (Reproduced with permission from Ref. [49], © Springer 2017).

Network electrical charge classification is based on the presence or absence of electrical charge on the hydrogel networks. This classification combines four groups, including non-ionic or neutral, ionic (anionic or cationic), amphoteric electrolyte and zwitterionic. Amphoteric electrolyte (ampholytic) comprises both basic and acidic groups. Zwitterionic, also known as polybetaines, encloses both cationic and anionic groups in each structural repeating unit.

2.3 Hydrogels preparation

For hydrogels prepared by crosslinking of one polymer to other polymers using appropriate crosslinker to form a 3D network, at least one polymer should be water hydrophilic. The cross-linker must be present to inhibit polymer chains dissolution before being applied, then the term "network" is inferred. No chains entanglement is observed in water-soluble polymers solution presented in low or intermediate concentrations. Moreover, the introduction of the cross-linker between chains of polymers will obtain a network with viscoelastic and purely elastic properties. There are two methods used for hydrogel preparation, namely chemical and physical methods. In physically crosslinked hydrogels, physical interaction is present between different polymer chains to prevent dissolution. In chemically crosslinked hydrogels, different polymer chains are connected by covalent bonds. Both methods will be discussed in the coming sections.

2.3.1 Chemically crosslinked hydrogels

The hydrogel can be obtained by several chemical crosslinking methods, including radical polymerization, chemical reaction with functional groups, irradiation with high energy, and reaction with the enzyme [52–55].

Radical polymerization method could be made with low molecular weight monomers in the presence of crosslinking agents [52, 56]. Moreover, the radical reaction occurs between a hydrophilic polymer with a polymerizable group and vinyl monomer using initiator and a crosslinking agent. Additionally, catalyst or initiator such as ultraviolet (UV) or microwave radiations helps to produce hydrogels [57, 58]. Several polymers, including synthetic, semi-synthetic and natural polymers, have been used in hydrogel preparation via radical polymerization. Poly(2-hydroxyethyl methacrylate) (pHEMA) hydrogel and poly(2-hydroxyethyl methacrylate)-co-polycaprolactone hydrogel (pHEMA-co-PCL) were synthesized by microwave assisted radical polymerization and atom transfer radical polymerization, respectively [59, 60]. In both hydrogels, PCL was used as a crosslinking agent, while the reaction initiator in the former was potassium persulphate. Both pHEMA and PCL polymers are biocompatible and biodegradable, and their hydrogels have been investigated for tissue engineering applications.

Kalia et al. reported guar gum-based superabsorbents hydrogel via free-radical aqueous polymerization [61]. They designed the hydrogel from guar gum (natural polymer) and itaconic acid monomer with hexamine and ammonium persulphate as a crosslinker and initiator, respectively. The authors also introduced polyaniline to the hydrogel network in order to increase the hydrogel conductivity. The synthesized hydrogel was found to be effective for dyes removal from waste-water and as an antibacterial agent against gram-positive bacteria.

Polymers with functional groups (–OH, –COOH, and $–NH_2$) possess the solubility properties, and these groups can be used for hydrogels formation. The reaction of polymers-functional groups with other corresponding group results in covalent crosslinking between polymers chains, such as Schiff base formation reaction or isocyanate-OH/NH_2 or amine carboxylic acid. A polymer with –OH groups could be crosslinked with an aldehyde to establish covalently crosslinked hydrogels, for example, glutaraldehyde used

to crosslink polyvinyl alcohol (PVA) with chitosan (CS) [53]. Additionally, structure modification of polymer is useful for hydrogel development. Sarika et al. have synthesized gum Arab-Gelatin hydrogel via Schiff base reaction and they modified gum Arab into aldehyde form by periodate oxidation, followed by crosslinking due to Schiff base reaction between the aldehyde of modified gum Arab with the amine group of gelatin [62].

Reactions between polymers functional groups could be conducted by addition reactions. Specifically, the functional groups of hydrophilic polymers react with bi-, tri- or higher functional crosslinking agents such as 1,6-hexanedibromide [63], 1,6-heaxmethylenediisocyanate [64, 65] and divinyl sulfone [66, 67]. The cleaning of hydrogels is required from traces of starting materials (unreacted cross-linkers, monomers, and polymers) after their preparation due to the toxicity issue. Another example, dextran-based hydrogels were synthesized by dual crosslinking with thio-modified serum albumin and poly(ethylene glycol) dithiol [68]. Dextran was modified with vinyl sulfone and crosslinked with thiolated albumin via Michael addition reaction, followed by addition of poly(ethylene glycol) dithiol to the mixture in order to enable the second crosslinking.

Polyesters and polyamides hydrogels are prepared by condensation reactions between hydroxyl or amine groups with a carboxylic acid. Gelatin and collagen-based hydrogels were synthesized by coupling reaction using water-soluble carbodiimide (EDC) and N-hydroxysuccinimide (NHS), and their swelling property can be controlled by crosslinker density [69, 70]. Additionally, polyfunctional carboxylic acids may be used in the condensation reaction of the polysaccharide-based hydrogel as crosslinking agents, such as citric, fumaric and malic acids [71, 72]. Specifically, in polyfunctional carboxylic acids, two carboxylic groups used in the condensation while the remaining groups serve as plasticizers to increase the swelling property [73]. Natural and modified polysaccharide-based hydrogel were fabricated using Isocyanide multicomponent reactions (Passerini and Ugi condensation). In Ugi reaction, diamine was used to crosslink with polymer carboxylic groups to achieve α-(acylamino)amide linkage, but Passerini method condensates the carboxylic groups with a dialdehyde (crosslinker) giving α-(acryloxy)amide [74, 75]. The chemical structure of hydrogels prepared through Ugi method marks it as more favorable compared to the other hydrogel due to stability at higher temperatures and different pH values [75].

Unsaturated compounds could be polymerized by high energy radiation such as gamma and electron beam. Therefore, the hydrogel preparation by crosslinking of vinyl groups derived from hydrophilic polymer chains can be conducted using high energy radiation [54, 76, 77]. Specifically, polymer irradiation results in the radical formation and allows the rearrangement of different polymer chains, and hence the covalent bond forms crosslinking network of the hydrogel. The irradiation is considered as the prominent method among others due to the absence of toxic chemical used during the process [54]. Furthermore, even without vinyl groups, a water-soluble polymer is capable of forming a hydrogel under high energy irradiation. Radical formed by C–H bonds homolytic scission through irradiation of polymers aqueous solutions, in addition to hydroxyl radicals generated from water molecules radiolysis could attack polymer chains to give macroradicals formation [23, 78]. Covalent bonds formed from macroradicals rearrangement with polymer chains could produce a crosslinked hydrogel. Carboxymethyl cellulose, poly(acrylic acid), poly(vinyl alcohol), poly(ethylene glycol), starch, and CS hydrogels had been prepared and crosslinked with high energy irradiation [79–84].

The enzyme-crosslinking method was demonstrated by Sperinde et al., where they fabricated PEG hydrogel with transglutaminase enzyme catalyzed the reaction between tetrahydroxy-PEG functionalized with glutaminyl groups (PEG-Q_a) and poly(lysine-co-phenylalanine) in aqueous solutions. The hydrogel network was formed by the amide linkage between the lysine ε-amine group and the γ-carboxamide group of PEG-Q_a. The higher swelling ratio of 90% was achieved on the synthesized hydrogel [55]. Moreover, the authors also synthesized another hydrogel by functionalizing PEG with lysine and crosslinking it with transglutaminase enzyme [85]. Recently, several hydrogels have been prepared by enzyme-crosslinking method [86–90].

2.3.2 *Physically crosslinked hydrogels*

Several physical crosslinking methods could be used to obtain hydrogel including hydrogen bonding, ionic bonding, molecular entanglements or physical interactions. Furthermore, physical hydrogel as well called "Temporary" hydrogel could be changed in their conformation such as shape due to environmental change or application by force and this change could lead to a reversible conformation [91, 92].

Ionic interactions method for the synthesis of physically crosslinked hydrogel can be established by the addition of metallic ions (Ca^{2+}, Fe^{3+}) to a polyelectrolyte solution [93]. Moreover, this type of crosslinking occurs in mild conditions, at physiological pH and room temperature [94]. Yang et al. reported that the use of trivalent cation like Fe^{3+} and Al^{3+} increased the strength of the hydrogel compared to that of using divalent cations like Ca^{2+} [95]. Alginate (Alg), a polysaccharide containing glucuronic and mannuronic acid groups, is the most well-known example of the ionic crosslinked polymer to design a hydrogel. Girgin et al. prepared alginate-gum Arab beads hydrogel with Ca^{2+} as multivalent cations using the ionic crosslinking method; the synthesized hydrogel is capable of delivering melatonin drug *in vitro* [96]. Another example of alginate hydrogel was synthesized by Rezvanian et al. where they produced alginate-pectin hydrogel using ionic crosslinked method for wood dressing applications [97]. Additionally, Gang et al. reported a new way of dual ions crosslinked of alginate/polyacrylamide hydrogel using barium and Fe^{3+} ions, producing a hybrid hydrogel with enhanced stiffness and strength due to dual metal ions used [98].

Hydrogen bonding interaction is an important method for fabrication and stabilization of biopolymers structures (DNA double helix). The hydrogen bonds formed by the protonation of carboxylic acids groups could form a pH-stimuli responsive hydrogel [52, 99]. Additionally, many tough and elastic polymeric hydrogels were constructed by hydrogen bonding [100–103]. Moreover, supramolecular polymer hydrogel of glycinamide-conjugated monomer was reported by Xiyang et al. using the cooperative hydrogen bonding crosslinking method with high mechanical strength due to dual amide effects [104].

Crystallization crosslinking method uses the sequencing process of freezing-thawing to produce a highly elastic and strong hydrogel. This method was discovered in 1975 by Peppas for the preparation of PVA hydrogels [105]. The hydrogel prepared by such method possesses properties that could be controlled by the polymer molecular weight, concentration of polymer, the time and temperature of freezing, and the freezing cycles number. Additionally, the polymer crystallites could act as physical cross-linker in the hydrogel, and the optimization of method conditions could produce a stable hydrogel for more than six months at 37 °C [94].

Crystallization crosslinking method could be used for homo-polymer hydrogels such as PVA hydrogels [52], and for the formation of stereocomplex systems. For example, opposite chirality of lactic acid oligomers is able to crosslink by crystallization method. Specifically, L-lactic acid and D-lactic acid are semi-crystalline homopolymers with melting temperature of 170 °C. Melting temperature of 230 °C is detected in a mixture of the high molecular weight of both homopolymers, which is ascribed to the stereocomplex formation [52, 94].

Amphiphilic block and graft copolymers methods are used to form a hydrogel; it makes polymeric micelles by a self-assembly process in aqueous media due to the aggregation of a hydrophobic chain of the polymers. The crosslinking occurs within graft copolymers or multiblock copolymers, where water-soluble polymer backbone from graft copolymers interacts with the hydrophobic segments [106]. The most known example of this crosslinking method is hydrogel prepared from poly(lactic acid) with PEG for drug delivery [107, 108]. Recently, Buwalda et al. reported diblock copolymer crosslinked hydrogels of PEG and poly(ε-caprolactone) for various biomedical applications [109]. Additionally, Hom and Bhatia design triblock copolymers hydrogels of alginate-clay nanocomposite with poly(ethylene oxide)-poly(propylene oxide)-poly(ethylene oxide) (PEO-PPO-PEO) for biomedical applications [110].

Physical crosslinking involves protein interaction for hydrogel preparation; a repetition blocks elastine-like and silk-like called ProLastins are components of block copolymers. In a water solution, ProLastins forms a fluid solution which under physiological conditions subjected to sol–gel transformation due to the crystallization of the silk-like domains [94]. Specifically, ProLastins is capable of being used as a carrier for drug delivery system. ProLastins were synthesized by Cappello and Tirrell, who pioneered protein engineering as a new field in materials chemistry [111, 112].

Additionally, antigen–antibody interactions had been used for the preparation of protein crosslinked hydrogels. Crosslinking agent like antibody could be grafted to an antigen, therefore during hydrogel swelling an exchange of the polymer bound antigen occurs, resulting in the release of antibodies along with free antigen presents in the solution, and decrease in the hydrogel swelling property. Immunoglobulin G (IgG) antibody grafted to poly(N-isopropylacrylamide), is an example of antigen–antibody interactions used in protein hydrogel preparation [113]. Moreover, recent research on physically crosslinked protein hydrogels has been reviewed [114].

The hydrophobic modification is the last method used in physical crosslinking hydrogels. Polysaccharides with hydrophobic segments modification are reported for the preparation of hydrophobic crosslinked hydrogels such as chitosan, carboxymethyl curdlan, pullulan, and konjac glucomannan [115–117].

3 Graphene oxide

3.1 Overview of production of graphene oxide from graphite

Graphite is 3D carbon material, made up of million layers of graphene. Graphite oxide is a multilayer compound of carbon, oxygen and hydrogen in different ratios with larger and irregular spacing, and could be obtained from graphite through an oxidation process. The earlier production of graphite oxide was using strong oxidizing agents, and the structure of the oxidized product has oxygenated functionalities, thus providing hydrophilic property and causes layer separation [118]. GO is a water-soluble oxidized form of graphene, and each single thick layer of GO consists of hydroxyl (OH), epoxide functional groups at two sides, while at the edges have carboxylic (COOH) groups. The difference between graphite oxide and GO is, that GO is single or a few layers system, while graphite oxide is a multilayer system (Fig. 4) [118, 119]. The method started by Hummers and Offeman involving potassium permanganate in concentrated acidic media is still the most common method used for GO synthesis [120]. Lerf-Klinowski and his group have presented the most conventional GO structure, supported by ^{13}C solid-state nuclear magnetic resonance (NMR) measurements [121]. In their model, epoxide and hydroxyl groups localize at the basal plane of GO sheet, while carboxylic acids or carboxylates are present at the sheet edges, and the functionalized groups provide hydrophilic

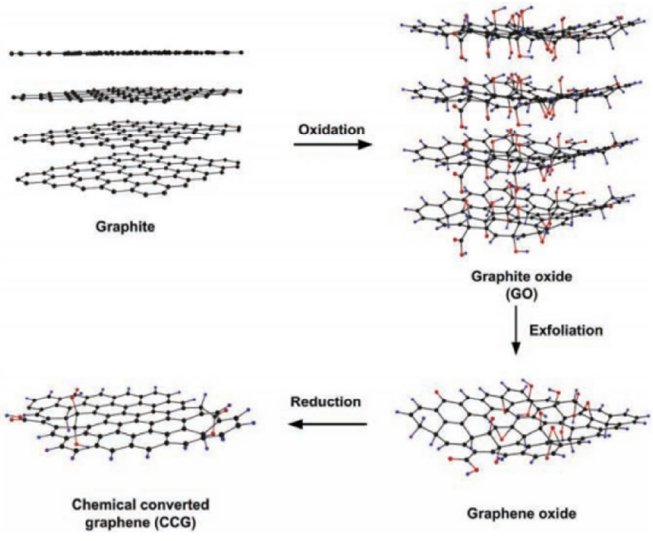

Figure 4 Preparation of graphene oxide from graphite (Adapted with permission from Ref. [118], © WILEY-VCH Verlag GmbH & Co. KGaA, Weinheim 2011).

characters (colloidal stability) and π-π interactions (π electrons of the sp^2 domain) [28, 122].

3.2 Graphene oxide hydrogels

The physicochemical properties of GO lead to its usage in many applications. Several GO hydrogels have been prepared through modification of GO functional groups with natural and synthetic polymers, enzymes, proteins, antigen and lysosomes by using chemical or physical methods. Chemical method occurs by covalent bonds formation with GO oxygen functional groups [123]. Amide bond was formed by introducing amino groups of CS to carboxyl groups of GO in order to prepare GO-CS hydrogel with improved properties for dyes removal [124]. Additionally, several polymers including PEG [125–127], PEI [128], amphiphilic copolymers [129], sodium alginate (SA) [130], and PVA [131] have been grafted to GO using the chemical method to improve their properties, such as decrease of cytotoxicity, and increase of hydrophilicity, stability, and cellular uptake.

On the other hand, the physical method occurs by non-covalent bond formation where the structure of GO is maintained. The non-covalent bond is formed by several kinds of interactions such as ionic bonds, hydrogen bonding, π-π stacking, coordination bonds, and van der Waals forces. Poly(sodium 4-styrenesulfonate) (PSS) was the first polymer material used for non-covalent interaction with GO to prevent the aggregation of GO sheets, where GO was reduced through exfoliation [132]. In addition, adamantine-grafted porphyrin was linked with folic acid (FA) -β-cyclodextrin and GO through π-π stacking interaction for organic molecules (pyrene, phenanthrene and naphthalene) adsorption from the water [133, 134]. Although, nanoparticles of Au have been loaded on GO through π-π stacking for inorganic molecules removal from water and aqueous media [135]. Hydrogen bonding can be formed between OH, COOH and other oxygen groups of GO with other materials, where no impurities are produced, and PVA have been grafted onto GO-glutamic acid (GO-Glu) through hydrogen bonding in PVA/GO-Glu nanocomposites hydrogel preparation for microbial removal in wastewater treatments [136]. Additionally, modified GO with non-covalent can be obtained using van der Waals interaction, such as FA conjugated with rGO for targeting drug delivery [137].

3.3 Cytotoxicity of graphene oxide in biomedical applications

The advancement in graphene synthesis, large-scale production and the succeeding of graphene-based biomedical development lead to rising in its exposure to humans and environments. Likewise,

before use of graphene in biomedical applications, an essential of systematic analysis of graphene biocompatibility is prerequisite. Accordingly, an enormous number of toxicological studies *in vitro* and *in vivo* have assessed the effect of graphene nanomaterials on different living systems including mammalian cells, animals and microbes models [138–146]. These studies reveal that several physicochemical properties affect the graphene cytotoxicity, including oxidative state, size, shape, synthesis method, dispersion state, functional groups, dose of administration, and exposure time [138–147]. A structure disruption and smaller carbonaceous fragments could be obtained after synthesis steps, or the synthesis method may lead to the formation of the final product with metallic impurities. Therefore, these perplexing factors could provoke mutable responses of toxicity [148–150].

Cytotoxicity assessment of graphene oxide and graphene have been carried out using several cell lines at different concentrations. A toxicity study on interaction of graphene (thickness 3–5 nm, diameter 100–110 nm) with PC12 cells of rat pheochromocytoma had been investigated and the results were compared with single-walled carbon nanotubes (SWCNTs) [151]. At high graphene concentration (100 μg/mL), significant lactate dehydrogenase (LDH) release was observed at 24 h of exposure to graphene, which indicates necrosis by membrane damage. However, graphene had no effect on the release of LDH at lower concentration (0.01–10 μg/mL), unlike SWCNTs which induced significant of LDH release. Morphology study also revealed the cell membrane remained intact after exposure to graphene. It proves that morphology of graphene offers lower cytotoxicity as compared to that of SWCNTs where its needle-like morphology could easily penetrate and damage cell membrane. It also showed that reactive oxygen species (ROS) were generated in a concentration- and time-dependent manner after exposure to graphene, indicating an oxidative stress mechanism. Additionally, graphene oxide cytotoxicity had been investigated on normal human lung cells (BEAS-2B) with dose range of 10–100 μg/mL and time exposure of 12 and 48 hours [152]. MTT assays showed an increase in the early and late apoptotic cells number beside a decrease in cell viability. Those results came out with dose- and time-dependent of GO cytotoxicity.

For cytotoxicity dependent of functional groups, a study was carried out on monkey renal cells for examination of pristine graphene and carboxylated GO cytotoxicity, at 10–300 μg/mL concentration range to compare the cellular interactions of hydrophilic and hydrophobic graphene derivatives [153]. The results showed an accumulation of pristine graphene on the membrane of cell led to F-actin alignment destabilization, while GO-COOH passed the cell membrane and accumulated in the region of perinuclear without any observation of membrane destabilization. All results pointed out that graphene nanoparticles with more oxidized functional groups can be cyto-compatible with an efficient delivery carrier at the intracellular level. Another study has been conducted for toxicity appraisal of GO and reduced graphene oxide (rGO) in human lung epithelial cells (A549) and mouse peritoneal macrophages (RAW 264.7) using fluorometric microculture cytotoxicity assay (FMCA), fluorometric DNA assay and MTT assay [154]. Around 0.0125–12.5 μg/cm^2 of GO and rGO concentrations were used for 5 days cell treatment and the result showed a dose dependent cytotoxicity. Additionally, there were connotation differences in cell death between GO, rGO and control, observed from the second day in A549 cells and the third day in RAW 264.7 macrophages at 1.25–12.5 μg/cm^2. There were no increases in ROS production when cell treated with low GO concentration besides intracellular accumulation of GO without any damage.

For size-dependent cytotoxicity of GO, different sizes of rGO (11 ± 4 nm, 91 ± 37 nm and 418 ± 56 nm) and GO (3.8 ± 0.4 μm) were used to investigate the cytotoxicity in human mesenchymal stem cells (hMSCs) using ROS assay, Comet assay, RNA assay and fluorescein diacetate assay [155]. The results showed that as the size of rGO increases, the percentage of death cells decreases. The same findings had been obtained for GO which indicates that the cytotoxicity of GO and rGO is size dependent.

Accordingly, to reduce the cellular toxicity of graphene oxide, surface functionalization process with biocompatible materials such as drugs, targeting molecules and polymers, could be employed. Yang et al. had systematically examined ^{125}I-labeled nanographene sheets functionalized with PEG for long-term *in vivo* biodistribution and its potential toxicity over time in female Balb/c mice using blood biochemistry, hematology and histology analysis [40]. The results showed no toxicity observed in female mice at the dose of 20 mg/kg. Biodistribution study also suggested that the functionalized graphene concentration reduced in most organs in mice after 3 days and it was gradually cleared from the mice, via both renal and fecal clearance. Hence, functionalization of GO with a biocompatible group may reduce the cytotoxicity at the cellular level and encourage graphene based *in vivo* biomedical research.

4 Graphene oxide hydrogels for anticancer drug delivery

GO attracts intense research interest in drug delivery community due to the presence of oxygen functional groups on GO edge surface for further functionalization. Moreover, GO is capable of stabilizing hydrophobic drugs due to amphiphilic properties and its large surface area renders it an excellent material for holding and delivering drugs by the π-π interaction between GO and drug aromatic groups. Several polymers (natural and synthetic) were combined with GO for hydrogel synthesis [156, 157], and the following sections will summarize the related GO hydrogels for anticancer drug delivery from previous literature.

4.1 Unmodified graphene oxide as anticancer drug carrier

Doxorubicin (DOX), an anticancer drug used for the treatment of several types of cancer disease such as breast, gastric and acute myeloblastic leukemia, had been loaded for the first time onto GO by Yang et al. [158]. They prepared this nanohybrid system by a simple physical method using sonication of GO and DOX in water at specific pH followed by overnight stirring at room temperature. The maximum DOX loading on GO was investigated by ultraviolet–visible (UV–Vis) spectrophotometer using standard DOX concentration curve at 233 nm wavelength, and DOX loading was found to be 2.35 mg/mg at initial DOX concentration of 0.47 mg/mL. The existence of hydrogen bonding between DOX and GO was confirmed by drug loading and release at different pH, where DOX possesses –OH and –NH_2 in their structure. Additionally, the results of electrochemical studies and fluorescent spectrum proved the existence of π-π stacking interaction. Yongnian et al. reported loading of 10-hydroxy camptothecin (HCPT) drug on GO as a method for serum albumin protein (BSA) analysis [159]. The authors proved the HCPT loading using the previously mentioned methods (fluorescence and electrochemical measurements) with atomic force microscopy (AFM) as supporting evidence. AFM showed that layers thickness of GO increased from 0.93 to 1.32 nm and the GO surface had granules shape which indicates the adsorption of CPT. Moreover, Wang et al. prepared GO nanocarrier for antihepatotoxic delivery, by incorporating glycyrrhizin (GL) with GO via hydrogen bonding interaction in aqueous solution [160]. The GL loading on GO was obtained as 5.19 mg/mg at initial GL concentration of 0.6 mg/mL. Additionally, the results showed that the prepared nanocarrier is pH-dependent, by showing drug release 58.4% and 17.6% at pH 5.5 and 7.4, respectively.

The effects of drug present in the GO interlayer had been studied

by Zhang et al. with DOX as a model drug [161]. Pyrolysis activation energy experiment was used via thermogravimetric analysis to assess the study and results showed a decrease in DOX-GO pyrolysis activation energy 26.3 w/w% as the DOX concentration on GO increased from 0 to 186.6%. It indicates that the π-π interactions between GO nanosheets were destroyed and a new π-π interaction formed between DOX and GO, whereas GO interlayer hydrogen bonding was blocked. Additionally, the authors provide evidence that during the drug loading, the drug prefers to employ the empty spot rather than multi-layers stacking on GO surface.

Without using polymers, Ma et al. had reported a strong and thixotropic GO hydrogel through mixing GO with DOX in aqueous solution at room temperature [162]. The gelation time could be reduced as the concentration of GO increased when introduced into DOX aqueous solution. A gel was formed and it encapsulated the DOX, which was proven by the tube inversion method (Fig. 5). Fluorescence spectroscopy, scanning electron microscopy (SEM) and X-ray diffraction (XRD) had been used to study the gelation mechanism. *In vitro* drug released study showed an enhanced drug activity with good profile behavior.

Zhou et al. demonstrated the co-loading of 7-ethyl-10-hydroxycamptothecin (SN-38) as CT drug and hypocrellin A (HPA), a photodynamic therapy drug, into GO drug delivery system [163]. Additionally, they also proved that the co-loading of drugs could solve the decrease in HPA activity when loaded alone on GO [164]. The biological evaluation showed a potential activity of HPA/SN-38/GO hybrid system compared to therapy system alone, therefore indicates that HPA/SN-38/GO is a promising hybrid therapy system for treatment of cancer cells. The solvent and co-solvent effect on thioguanine drug-loaded GO had been studied by Hasanzade and Raissi by using molecular dynamics simulation and density functional theory (DFT) [165]. Thioguanine is an anticancer drug used to treat the acute myeloid leukemia. DFT calculations showed that GO-thioguanine adsorption is made via interactions of the hydrogen bond. Moreover, water solvent was found to be the suitable medium for the interaction of drug on GO. Overall results revealed that GO is a good nanocarrier for anticancer drugs.

4.2 Chemically crosslinked graphene oxide hydrogels for anticancer drug delivery

Covalent bonds are formed via chemical crosslinked method and this method could involve several reactions to prepare GO hydrogels such as radical polymerization, chemical reactions with functional groups, irradiation with high energy, and reaction with enzyme.

4.2.1 Radical polymerization method

Bardajee and Hooshyar reported thermo-response nanogels (TNGs) of salep-modified GO with N-isopropylacrylamide (NIPAM) through radical polymerization method (precipitation and dispersion) using *N*,*N*-methylenebisacrylamide (MBA) as a crosslinker and ammonium persulfate (APS) as initiator [166]. Doxorubicin (DOX) was chosen as a model drug, and salep is a polysaccharide that has a similar structure to CS and gelatin. It mainly consists of glucomannan with linear structure of mannose and glucose bonded together by glycosidic bonds of β-(1 → 4). Salep is nutrient-rich material that used in food formulations and hydrogel synthesis for drug delivery. Specifically, the authors synthesized the TNGs through three steps as shown in Fig. 6. The first step is GO synthesis, followed by mixing with salep. The final step involved the addition of MBA, NIPAM, and APS for radical polymerization reaction under Ar atmosphere at 70 °C to produce TNGs. The final product was washed with water to remove unreacted materials, dried at room temperature and grounded to uniform size particles. Drug loading showed about 77% loading and a good drug release of TNGs, thus offering an excellent nanocarrier in the presence of GO. Additionally, the thermal studies showed the slow drug release at lower temperatures, but at higher temperatures, the drug release significantly increased due to the presence of thermo-responsive material (NIPAM) in nanogels.

In 2014, Chen et al. synthesized double network GO hydrogel through two steps method in order to deliver anticancer drug [167]. In the first step, GO was modified with β-cyclodextrin (β-CD) using hydrothermal reduction method, followed by radical polymerization with *N*,*N*-dimethylacrylamide (DMAA) in the presence of APS as initiator and *N*,*N*,*N*',*N*'-tetramethylenediamine as a crosslinker. Additionally, camptothecin (CPT) was selected as model drug and control experiment was conducted with graphene hydrogel without β-CD. Fourier transform infrared spectroscopy (FTIR) and SEM had been used for functional group characterization and surface morphology studies, respectively. Results showed that CPT drug loading was higher in GO-β-CD than control GO hydrogel. Drug released profile showed that control GO hydrogel released CPT faster in the first 2 hours and CPT accumulation was 55%, while GO-β-CD released CPT slower and linear in the first 7 hours with 70% CPT accumulation. Overall results indicated that GO-β-CD is a promising scaffold nanocarrier for an anticancer drug.

Moreover, Zhang et al. had combined chemical and physical methods for compressed strength preparation of ternary GO hydrogel with polyacrylamide (PAM) and carboxymethyl cellulose (CMC) [168]. The chemical method started by free radical polymerization of acrylamide (AM) with GO and CMC in aqueous solution using *N*,*N*-methylenebisacrylamide (MBA) crosslinker and APS as an initiator. In the physical method, aluminum ion was used for CMC crosslinking (see Fig. 7). The ionic bond formed between GO oxygens functional groups and N–H of PAM was confirmed by FTIR analysis, and the compressive strength was found to be 2.87 MPa. Additionally, the presence of GO enhanced the mechanical strength, which influenced the swelling behavior of ternary hydrogels. The findings render ternary GO hydrogels as the excellent candidate in drug delivery and bioengineering.

Atomic transfer radical polymerization (ATRP) has been used to prepare a nanocarrier of GO-poly(N-vinyl caprolactam) (PVCL)

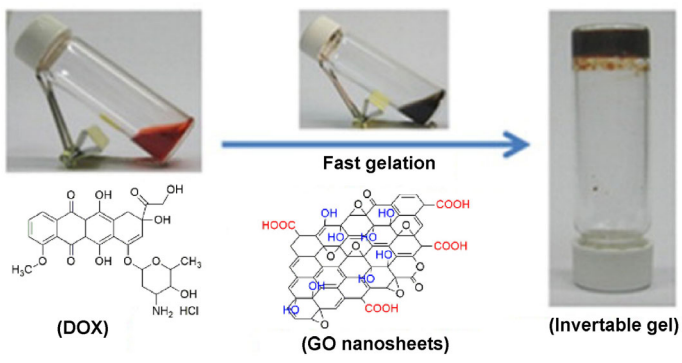

Figure 5 GO-DOX hydrogel formation. (Adapted with permission from Ref. [162], © Elsevier Ltd. 2012).

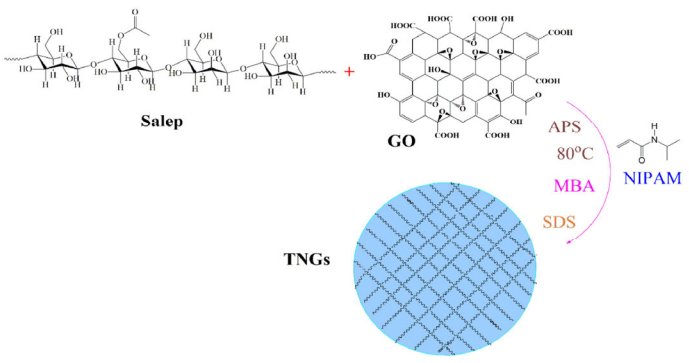

Figure 6 TNGS preparation scheme (Adapted with permission from Ref. [166], © Springer 2017).

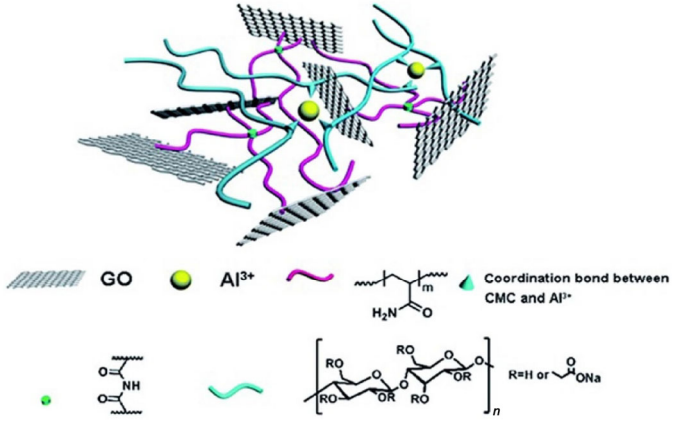

Figure 7 GO/PAM/CMC schematic structure (Adapted with permission from Ref. [168], © Royal Society of Chemistry 2014).

for anticancer drug delivery [169]. The radical initiator was firstly incorporated on GO by modifying GO with NH_2 group using diaminopropane, NHS and N-(3-(dimethylamino) propyl)-N'-ethylcarbodiimide hydrochloride (EDC.HCl) in an aqueous medium, followed by the addition of 2-bromo-2-methylpropionyl bromide to produce GO modified with Br as ATRP initiator. Radical polymerization was carried out using *N*,*N*,*N*,*N*,*N*-pentamethyldiethylenetriamine (PMDETA) and N-vinyl caprolactam (NVCL) to yield PVCL-grafted GO (Fig. 8). CPT was selected as a model drug with high loading of 20%, and the drug release profile had shown GO-PVCL is pH-responsive with temperature-controlled targeted delivery. *In vitro* studies exhibited the ability of GO-PVCL for damaging cancer cell with no observed toxicity. This results revealed the biocompatibility and stability of GO-PVCL. Kundu et al. had reported a fluorescent nanocarrier of GO-poly(N-isopropylacrylamide) via radical polymerization for delivery of hydrophilic and hydrophobic anticancer drugs [170]. Additionally, several GO scaffolds had been formulated using radical polymerization method as listed in Table 1.

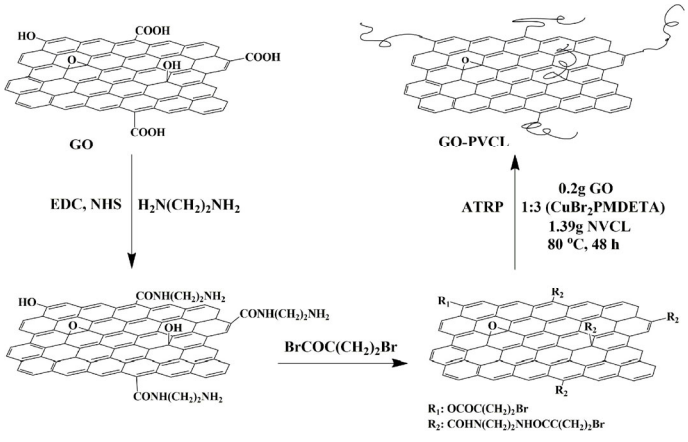

Figure 8 GO-PVCL schematic synthesis (Adapted with permission from Ref. [169], © Elsevier Ltd. 2014).

Table 1 Covalently bonded GO nanocomposites fabricated via radical polymerization[a]

GO nanocomposites	Model drugs	Drug loading capacity (%)	Ref.
Fe_3O_4@mSiO_2@GO-HeA-PEG-SA	DOX	21.00	[171]
PMAA-GO	Naproxen	37.00	[172]
PMAA-GO-PEG	DOX	57.40	[173]
GO-Heparin	DOX	68.90	[174]
Salep-GO-P(NIPAM-co-AA)	DOX	72.00	[175]

[a]PMAA = poly(methacrylic acid), HeA = hexamine, P(NIPAM-co-AA) = poly(isopropylacrylamide-co-acrylic acid).

4.2.2 *Method of irradiations with high energy*

A pH-responsive hydrogel had been prepared by copolymerization and crosslinking of GO, SA and acrylic acid (AAc) using gamma irradiation [176]. SA is a natural polymer and Cefadroxil was used as a model drug. GO/(AAc-co-SA) hydrogel synthesis started with GO preparation based on modified Hummers' method, then AAc and SA were mixed in the GO solution, followed by irradiation of ^{60}Co gamma rays (20 kGy, 10.28 kGy/h) for 117 min. The fabrication of GO in GO/(AAc-co-SA) hydrogel matrix was characterized, and swelling measurements showed that presence of GO in hydrogel enhanced and regulated the swelling at different pH buffer solutions (pH 1 and 7). Profile study of drug release gave promising results as a proof that the GO/(AAc-co-SA) could be used for the drug delivery system.

4.2.3 *Reaction with enzyme method*

Dai et al. synthesized novel low-temperature hydrogel of CS/GO using β-glycerophosphate (GP) enzyme as a crosslinker and Tris(2,2′-bipyridyl)dichlororuthenium(II) was loaded as an anticancer drug [177, 178]. The scaffold was prepared through a simple mixing of GO, CS and GP at different ratios with the addition of acetic acid to enhance CS solubility. GP have been reported to have a unique property by keeping the CS solution in a liquid state at physiological pH but tend to become gel when heating at physiological temperature. The gelation time and temperature studies showed that the increase of GP concentration reduced the gelation temperature. Additionally, the increase of GO concentration reduced the gelation temperature up to 33 °C and gelation time up to 9 min. The study of drug release profile showed that the scaffold improved the drug delivery as compared to control experiment CS hydrogels.

Additionally, an injectable hydrogel has been reported by Lee et al. by *in situ* enzymatic crosslinking of 4-arm polypropylene oxide (PPO)-polyethylene oxide (PEO)-tyramine (Tet-TA) with different oxidation levels of GO [179]. X-ray photoelectron spectroscopy (XPS) and FTIR characterizations showed the increment in the oxidation level of GO and surface area of GO. The presence of Tet-TA enhanced the dispersibility while the GO improved mechanical property of hydrogel. It was found that this hybrid scaffold is biocompatible and non-toxic, suggesting it to be used as injectable hydrogel for drug delivery and tissue engineering.

4.2.4 *Reactions with functional groups method*

An example on chemically crosslinked GO hydrogel via reaction with functional groups had been demonstrated by Yang et al. by fabricating composite GO hydrogel with carboxymethyl chitosan (CMCS), hyaluronic acid (HA) and fluorescein isothiocyanate (FI) [180]. This hydrogel was prepared in two steps, starting with modification of GO with CMCS via amide linkage between $-NH_2$ group of CMCS and –COOH of GO, followed by conjugation of the amino group in GO-CMCS with carboxylic groups of HA and FI to form the final scaffold (GO-CMCS-FI-HA) (Fig. 9). The hydrogel scaffold was confirmed by FTIR and transmission electron microscopy

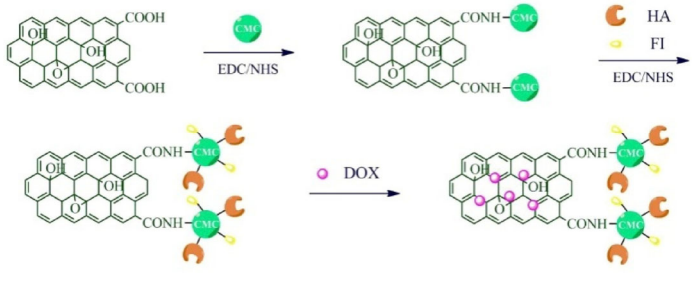

Figure 9 GO-CMCS-FI-HA hydrogel synthesis scheme (Adapted with permission from Ref. [180], © Elsevier Ltd. 2016).

(TEM) [180]. DOX was used as a model drug and capacity of drug loading was 95%. Drug release profile study showed the optimum drug release occurred at pH 5.8, rather than pH 7.4. Biological evaluation of hydrogel cytotoxicity on HeLa cells gave no toxicity, which revealed that this scaffold is a potential nanocarrier for targeted anticancer drug delivery.

GO-PEG nanocomposites had been reported for paclitaxel (PTX) anticancer drug delivery [181]. This nanocomposite prepared via amide linkage process with six armed PEG was functionalized with amine groups followed by a condensation reaction in an aqueous medium at room temperature. AFM analysis displayed GO-PEG particle size ranged 50–200 nm. Bioassay showed the biocompatibility and nontoxicity of GO-PEG of A549 and MCF-7 cell lines. PTX was conjugated with GO-PEG via hydrophobic interactions and π-π stacking, and the drug loading capacity was 11.2 wt.%. Biological evaluation on A549 and MCF-7 revealed the cytotoxicity of GO-PEG/PTX nanocomposites with greater penetrability as compared to PTX itself. Moreover, inverted fluorescein microscopy supported the GO-PEG/PTX nanocomposites cytotoxicity using FI investigation.

Wu et al. had synthesized a covalently bonded heparin-GO (Hep-GO) nanocarrier via click chemistry reaction [182]. GO and heparin polysaccharide were functionalized with azide group and proparglyamine, respectively. DOX and granulocyte colony-stimulating factor (G-CSF) were selected as a model drugs. G-CSF was used after the CT treatment in order to recover the white blood cells after treatment, or before the CT treatment to stimulate bone marrow for the production of stem cells. Hep-GO colloidal stability in aqueous solution was studied using UV–Vis spectroscopy. *In vitro* study showed that Hep-GO/DOX/G-CSF had high thermal stability and the drug was released at a long period of time with lower drug cytotoxicity. Overall results, promote Hep-GO as a potential nanocarrier scaffold for multi-anticancer drugs.

A nanocarrier for anticancer drug and gene co-delivery has been fabricated using GO functionalized with polyamidoamine dendrimer (GO-PAMAM) [183]. PAMAM was synthesized through three generations by Michael addition polymerization of ethylenediamine and methylacrylate, where propargylamine was used as the polymer core. GO was coupled with PAMAM via amide linkage in the presence EDC.HCl and NHS (Fig. 10). DOX and MMP-9 shRNA (gene) were loaded into GO-PAMAM with high capacity. Cell counting kit-8 (CCK-8) bioassay study showed lower cytotoxicity of GO-PAMAM compared to traditional gene carrier PEI-25k. The biological study on MCF-7 cells revealed that GO-PAMAM had high biocompatibility and good drug release profile with better transfection efficiency than PEI-25K, in addition to substantial inhibition of the MMP-9 protein expression inside MCF-7 cells. Hence, all results promoted GO-PAMAM as drug-gene dual nanocarrier. More GO based hydrogel produced by chemical crosslink are summarized in Table 2.

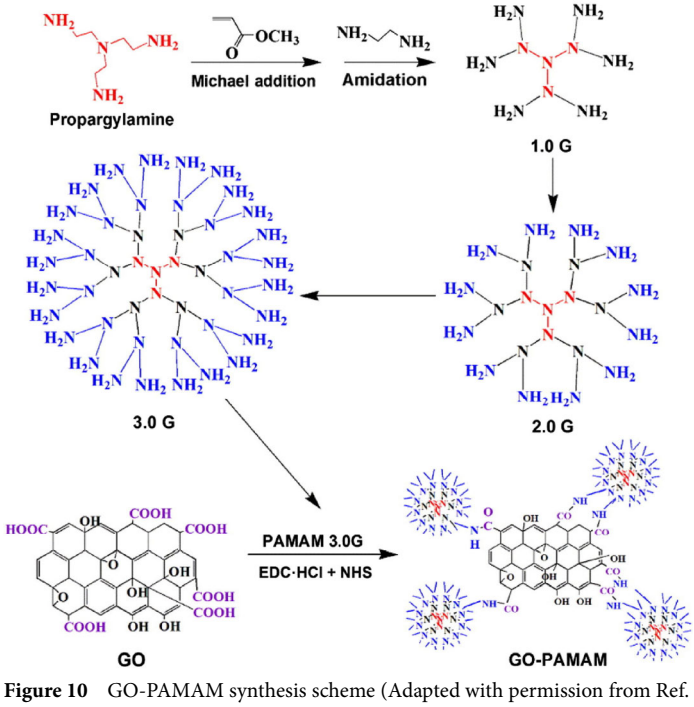

Figure 10 GO-PAMAM synthesis scheme (Adapted with permission from Ref. [183], © Elsevier Ltd. 2017).

4.3 Physically crosslinked graphene oxide hydrogels for anticancer drug delivery

The physical crosslinked GO hydrogels are predominantly formed by several physical methods such as hydrogen bonding, ionic bonding, crystallization, protein interactions and hydrophobic interactions.

4.3.1 Crystallization method

The crystallization method was used to prepare hyperbranched polyglycerol-GO (HPG-GO) hydrogel as an anticancer drug carrier with DOX as a model drug [202]. This hydrogel was synthesized using anionic ring-opening polymerization of HPG with GO and deprotonation was done with potassium hydride and 18-crown-6, followed by continuous freezing-thawing cycles to obtain the matrix as a final product (Fig. 11). Drug profile studies showed that this hydrogel was biocompatible and capable to deliver the drug with high cytotoxicity. Specifically, the blood compatibility studies also revealed that this hydrogel has an insignificant effect on blood clotting and hemolysis.

4.3.2 Hydrogen bonding interactions method

Using hydrogen bonding methods, Hu et al. synthesized a supramolecular hydrogel of GO/Graphene-Pluronic F-127 for the delivery hybrid drugs of CPT and DOX [203]. Pluronic F-127

Table 2 Covalently bonded GO nanocomposites fabricated via functional group reaction[a]

GO nanocomposites hydrogel	Model drugs	Drug loading capacity (%)	Ref.
DOX-SS-GO-Ag	DOX	253.50	[184]
GO@ $mSiO_2$-CS	DOX	21.00	[185]
GO-AADH-HA	DOX	81.50	[186]
GO-ALG	5-FU	32.53	[187]
GO-CMCS-FI-LA	DOX	96.00	[188]
GO-COO-HP-β-CD	PTX	29.93	[189]
GO-CS-SA	DOX	70.19	[190]
GO-mPEG	RV	78.80	[191]
GO-N=N-GO/PVA	CUR	20.64	[192]
GO-PAA	DOX	92.70	[193]
GO-PEG-HA	DOX	90.00	[194]
GO-PEI-FI-PEG-LA	DOX	85.00	[195]
GO-PLA-PEG	PTX	11.00	[196]
GO-SA	DOX	184.30	[197]
GO-SS-SA	DOX	97.00	[198]
PEG-GO	BER	75.00	[199]
PLA-PEG-PLA/(CS-GO)	DOX	110.00	[200]
α-CD@PEG-g-CS-Fe_3O_4@GO@$mSiO_2$	DOX	19.00	[201]

[a]HA = hyaluronic acid, AADH = adipic acid dihydrazide, mPEG = methoxy-polyethyleneglycol amine, RV = resveratrol, PAA = poly(acrylic acid), α-CD = α-Cyclodextrin, PLA = poly(lactide), BERr = berberine, GO-COO = carboxylated Graphene oxide, HP = hydroxypropyl, LA = lactobionic acid, CUR = curcumin.

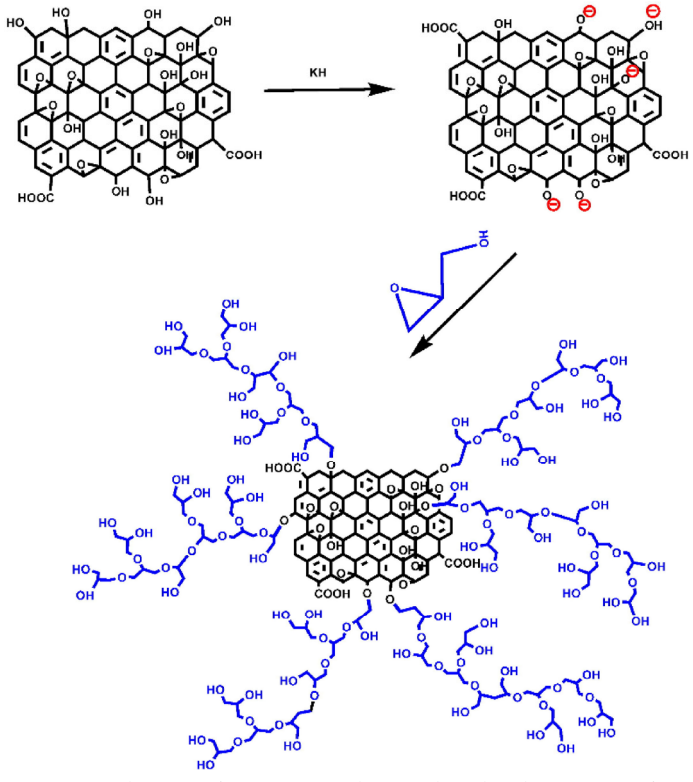

Figure 11 Schematic of HPG-GO synthesis (Adapted with permission from Ref. [202], © Elsevier Ltd. 2017).

is biocompatible triblock copolymers of poly(ethylene oxide)-poly(propylene oxide)-poly(ethylene oxide) that obtained food and drug administration's (FDA) approval, possesses thermal sol-gel transition property [137]. Hydrogel synthesis was started by mixing of GO with Pluronic F-127 in 1:25 ratio to form Pluronic functionalized-GO, then additional Pluronic copolymer where crosslinked with GO using α-CD as a crosslinker to produce GO/graphene-Pluronic hydrogel. Drug loading profile showed the GO/graphene-Pluronic hydrogel capability to load more drugs compared to the native hydrogel. These results pointed out its suitability as injectable hydrogels for anticancer drugs delivery.

A pH-responsive hydrogel of Konjac glucomannan-GO (KGM/GO) was prepared in different ratios as a nanocarrier for 5-aminosalicylic acid (Mesalazine) anticancer drug [204]. KGM-carboxylic groups were first converted into hydroxyl groups through sodium carbonate treatment, followed by mixing with GO at 90 °C for one hour and frozen for 24 hours to produce KGM-GO. The hydrogen bonds were formed between hydroxyl groups of KGM and carboxylic groups of GO. Additionally GO had enhanced the swelling and thermal stabilities of KGM-GO nanocomposites. Drug release profiles showed an initial burst effect, hence KGM-GO is not a perfect carrier for mesalazine delivery.

4.3.3 *Hydrophobic interactions method*

Oil-water emulsion method (hydrophobic interactions) was used to prepare pH-stimuli response injectable nanoparticles hydrogel composed of acetated-β-CD (Ac-β-CD) and GO with CPT as a model drug [205]. The results of drug release study showed the drug release change as the pH changed due to the Ac-β-CD hydrolysis. *In vitro* biological study gave a controllable drug release from the injectable hydrogel. Additionally, dynamic mechanical test and SEM characterization proved the mechanical properties and the structural property of the scaffold.

A hydrophobic interaction and π-π interactions were found between CS and GO in CS-β-GP-GO nanocomposites hydrogels, apart from the ionic bonds in CS-β-GP, where CS was modified with β-glycerophosphate (β-GP) to make thermosensitive gels [206]. Swelling measurements showed a higher swelling ratio due to the presence of GO and the higher porosity of GO-CS. Bioassay study on 3T3 cells revealed the lower cytotoxicity of the bare nanocomposite hydrogels compared with non-GO hydrogels. Methotrexate (MTX) anticancer drug release profile from nanocomposite hydrogels was studied on MCF-7 breast cancer cell and showed the capability of nanocomposite hydrogels to delivery anticancer drug with prospective controllable therapy without side effect.

4.3.4 *Protein interactions method*

Tian et al. used protein interaction method for the synthesis of GO based-PEGylated folate nanocarrier via peptide bond for CPT drug delivery [207]. The nanocarrier synthesis was done by sonication of GO in the presence of EDC and NHS, then GO was mixed with folate-polyethylene glycol–amido (FA-PEG_{2000}-NH_2) and methoxy-polyethylene glycol–amido (Me-PEG_{2000}-NH_2) to obtain the nano-carrier. Drug loading showed capacity of more than 1.7 mg/mg (90% efficiency), and the cytotoxicity assay and MTT revealed the ability of the nanocarrier to load and release the anticancer drug to the folate-receptor in cancer cells without any side effect on the normal cells.

4.3.5 *Antigen-antibody interactions method*

PEI-GO nanocomposite was prepared in order to deliver a nonviral gene of small interfering RNA (siRNA) and transfect against C-X-C chemokine receptor type 4 (CXCR4) in breast cancer cells [208]. CXCR4 is known as G protein-coupled receptor in cancer metastasis and migration. Therefore, Anti-CXCR4 or siRNA, is used to suppress CXCR4 and prevent cancer cells metastasis and migration. PEI-GO particle size was increased from 188 to 262 nm when the temperature rose from 25 to 37 °C. Electrophoretic mobility shift assay (EMSA) was used for siRNA incorporation into PEI-GO nanocomposites. Biological evaluation on MDA-MB-231 breast cancer cell showed a transfection, suppression and inhibition against CXCR4 using PEI-GO/siRNA nanocomposites. Moreover, real-time PCR and western blot analysis were used to confirm and support the results. Consequently, PEI-GO scaffolds are considered as an active nanocarrier for siRNA for targeting and gene therapy of cancer metastasis.

Dopamine (DA), a neurotransmitter of monoamine and catecholamine possesses a substantial role in brain central nervous system. There are DA receptors in cancer cells which could be overexpressed in breast cancer cell and human colon adeno-carcinoma. Masoudipour et al. reported DA-GO as a nanocarrier for MTX anticancer drug and targeting the DA receptor in cancer cell [209]. The DA-GO hydrogel was prepared by using a simple method of DA conjugation with GO in the presence of EDC and NHS, followed by changing all epoxy and hydroxyl groups of GO into carboxylic acid groups via the addition of chloroacetic acid in basic medium. The particle size of DA-GO/MTX was 342.7 nm and MTX drug loaded capacity was 19.72%. Biological evaluation on MCF-7 breast cancer cell showed a controllable target to DA receptor positive cell with insignificant cytotoxicity effect on DA receptor-negative cells.

Dextran-GO had been decorated by AS1411 Aptamer (GODEX-Apt) as a nanocarrier for CUR drug [210]. AS1411 Aptamer is anti-nucleolin, oligodeoxynucleotide aptamer of 26-base guanine-rich, owning a potential apoptotic induction activity. It targets the nucleolar phosphoprotein called nucleolin, located on the surface of cancer cells with high overexpression. Therefore, AS1411 prevents nucleolin to bind mRNA of anti-apoptotic called BCL2, hence destabilizing BCL2 mRNA and cuts off protein synthesis of BCL2, results in apoptosis induction. The π-π stacking interactions were observed between CUR anticancer drug and GO-DEX-Apt, and the

drug loading capacity was 29%. Biological studies on 4T1 and MCF-7 cancer cells revealed the penetrability of nanocarrier to cancer cells with high efficiency and significant cytotoxicity.

Another nanocarrier was fabricated for targeting folate-receptor in cancer cells using GO decorated with folic acid-grafted serum albumin. DOX was used as a drug model with a loading capacity of 43.7% [211]. Deb and Vimala studied the effect of natural and synthetic polymer on folic acid-GO nanocomposites for CPT delivery and targeting folate receptor in cancer cells. CS was used as a natural polymer and polyvinylpyrrolidone as a synthetic polymer. Their studies reported that natural polymer-GO was more suitable nanocarrier for CPT drug with higher loading capacity and greater inhibition based on MTT and SRB assay [212]. Furthermore, Cui et al. synthesized multistimuli-responsive nanocarrier of magnetic GO functionalized with folic acid for targeting drug delivery using Cumarin 6 as a model drug [213].

4.3.6 *Ionic interactions method*

A novel carrier of CMCS/GO hydrogel was synthesized by ionic interaction method using Ca^{2+} [214]. Hydrogels composites were mixed in an aqueous medium, followed by micro-dropping into $CaCl_2$ solution to solidify the hydrogel particles (Fig. 12). The average CMCS/GO particle size was 275 μm, and these particles were found to be stable in NaCl solution for more than one week. Drug loading profile experiments displayed the efficiency of the hydrogel to adsorb several drugs, such as DOX and bovine serum albumin, with high 0.45 mg/mg loading capacity and better releasing profile. The overall results indicated that the CMCS/GO hydrogel is a promising carrier for drug delivery.

Wang et al. synthesized KGM-SA-GO nanocarriers to control 5-FU anticancer drug release [215]. GO was used as drug binder because it has a large surface area with epoxy and hydroxyl groups for drug π-π stacking and hydrogen bonding interactions, SA was used as pH-stimuli response agent and KGM as a matrix to make more stable hydrogel. To facilitate KGM interaction with SA in the GO scaffold, KGM was treated in alkali solution (pH 8) at 90 °C in the presence of SA, GO and Ca^{2+} ions for deacetylation and crosslinking process. 5-FU drug loading capacity was 32.04%, and the study of drug release profile was conducted in different buffer solutions (pH 1.2 and 6.8) to simulate the stomach and colon physiological conditions. Results showed that controlled drug release was achieved without any matrix burst. The overall result showed GO was better binding effector in nanocarrier matrix for delivery of anticancer drugs.

A hybrid microcapsule of magnetic GO-SA-CS-HA for anticancer drugs delivery and CT systems was reported by Deng et al. [216].

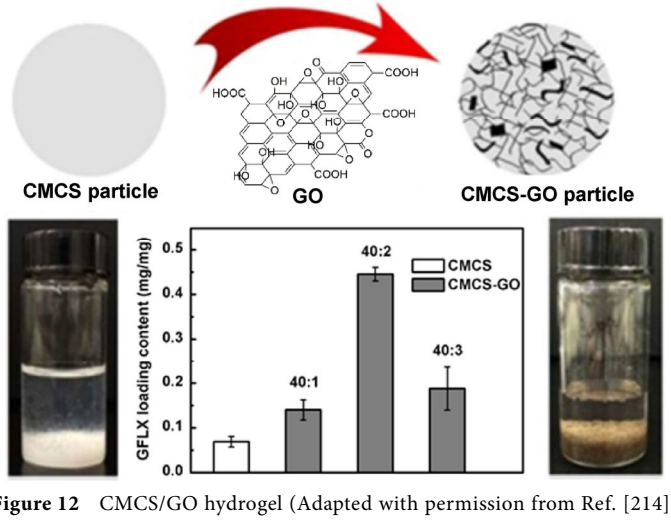

Figure 12 CMCS/GO hydrogel (Adapted with permission from Ref. [214], © Springer 2016).

This microcapsule was prepared using layer-by-layer method, starting with co-precipitation of iron oxide-GO (Fe_3O_4@GO), followed by layer-by-layer microcapsulation of polysaccharides including SA, CS and HA. The ionic interaction between polysaccharides and the magnetic Fe_3O_4@GO was monitored by zeta potential measurements. Fe_3O_4@GO particles size was 191.2 nm with zeta potential of −14.2 mV which indicated the higher stability and interactions between layer and Fe_3O_4@GO. Morphological study of microcapsules showed the distribution of Fe_3O_4@GO in the microcapsule. Additionally, bioassay study on HeLa cells came with non-toxicity issues due to the biocompatibility of polysaccharides. DOX was engaged as a model drug with 13.2% loading efficiency. *In vitro* and *in vivo* antitumor activity studies showed high controllable and synergistic result, thus supporting GO microcapsules to be a promising nanocarrier for hybrid treatment system of drug delivery-CT.

Clinoptilolite (Clin) was functionalized with zinc and GO (Zn-Clin-GO) as a nanocomposite for anticancer drug delivery [217]. Clin is a natural zeolite with biocompatible property. In nanocomposites preparation, cations in Clin were first replaced with Zn^{2+} in NaCl solution, then GO and Zn-Clin were mixed and dispersed in deionized water followed by $NaBH_4$ addition and hydrothermal treatments to obtain Zn-Clin-GO nanocomposite. Bioassay on A549 cells showed that Zn-Clin-GO had no obvious cytotoxicity with very high cell viability. DOX drug loading capacity was very high (90%) in 30 min. Study of drug release profile in different pH buffer solution (pH 5.4 and 7) demonstrated slow drug release from Zn-Clin-GO. The authors concluded that this nanocomposite has the capability to be a drug carrier.

Recently, nanocomposite hydrogel beads of CMC-GO were prepared through Fe^{3+} ion crosslinking method for DOX drug carrier and release system [218]. FTIR, TEM and SEM were used to confirm the GO nanocomposite beads formation. DOX loading capacity was high due to π-π stacking interaction between DOX and GO. Moreover, the drug release profile in buffer solutions at pH 1.2 and 6.8 was controlled and pH-dependent.

CS-GO nanocomposites were prepared via electrostatic interactions for carrying and intracellular delivery of CpG oligodeoxynucleotides (CpG ODNs) [219]. CpG ODNs is an immunotherapeutic agents activate immune responses, where CpG refers to "C", a cytosine triphosphate deoxynucleotide, "G", a guanine triphosphate deoxynucleotide, and "p" refers to the phosphodiester link between C and G. CS-GO scaffolds enhanced the CpG ODNs loading and cellular uptake, and enriched the production of the tumor necrosis factor-α (TNF-α) interleukin-6 (IL-6). Consequently, CS-GO nanocomposite is a promising nanocarrier for CpG ODNs.

Sudhakar et al. had reported GO-poly(N-isopropyl acrylamide)-SA (GO-PNIPAM-SA) nanocomposite hydrogel beads crosslinked via Ca^{2+} ions with dual pH and temperature response property for delivery of 5-FU anticancer drug [220]. The beads showed high drug encapsulation efficiency (90%) with slower drug release profile (> 32 hours) with no burst release and non-obvious cytotoxicity. Thus, it had the capability to be used for anticancer drug controlling release carriers.

Moreover, a 5-FU nanocarrier hybrid aerogel had been prepared via Ca^{2+} crosslinking of CS, CMC with GO [221]. Specifically, a solution of GO, CMC, Ca^{2+} and CS were mixed well and adjusted to pH 7 for the precipitation of hybrid hydrogels. Owing to the pH sensitivity of CS and SA, the drug release (5-FU) of this aerogel was examined under different pH using Higuchi model and Korsmeyer-Peppas model. The pH controlled drug release could be achieved by this nanocarrier hybrid aerogel.

5 Nano-bio interfaces of graphene oxide

Carbon nanomaterials, without doubt are the most celebrated

products of nanotechnology to date. These nanomaterials can enter the human body through inhalation, skin contact, ingestion or injection, thus creating multiple questions need to be answered. The study on interface between nanomaterials and biological components is the gateway for understanding biological response towards nanomaterials. The different surface chemistry of nanomaterials could produce significant differences in the biological response [222–225].

The interactions of GO with biological molecules can be demonstrated in several ways, including small molecules and ion adsorption, DNA/RNA interactions, catalysis of oxidative reactions, and protein and lipid interactions [226]. For small molecules and ion adsorption, GO has a high surface area capable to adsorb small molecules from physiological fluids which are partially hydrophobic, low soluble, or positively charge (GO possesses negative charge), and having π bonds conjugation which easily interact with GO surface by π-π stacking [227, 228]. Thus, the biological relevant may include objects in assays which depend on dyes-based molecular investigations [229], small drug loading capacity [230], deficiency of micronutrient [227], and the toxicity effects of antagonist or synergist objects when GO and small toxic molecule coexist, and their bioavailability is controlled by the partition to GO surfaces [231]. GO-based carriers for drug delivery are related to small molecules interactions [232].

In DNA/RNA interactions, graphene families (with small lateral dimension) have unique modes to intercalate with DNA and RNA [233, 234]. Specifically, they preferred the adsorption of single-stranded other than double-stranded forms, and this protects the adsorbed sites from any nuclease enzymes attacking [233]. The physicochemical properties of GO make it to be attractive in delivery and sensing of DNA and RNA, where the interactions of GO-DNA bases in ssDNA are hydrophobic and π-π stacking, knowing that DNA is polyanion [234]. The explanations behind that, π-π stacking forces can overcome the electrostatic repulsion between GO and polyanion of DNA, specifically when ionic strength is high, and the charges are shielded by electrolytes, or at low pH where protonation reduces the GO charge [235]. The bases in dsDNA are protected by double helix, and the charged phosphate groups, which are located at the outer double helix, has low affinity to GO surfaces [235–237].

In oxidative reactions, GO shows significant catalytic activity in this type of reactions, where the surface of GO generates ROS, as an intermediate way to the reduction process of molecular oxygen to water [238, 239]. GO is able to deactivate the antioxidant glutathione through catalyzing the reaction of glutathione with O_2 [240]. In addition, it is facilitating the oxidative damage in living cells, therefore an advantage for GO in cancer cell therapy [241].

The adsorptions of protein on the GO surface is facilitating the way to cellular uptake and hence responses to toxicity [145]. GO possesses larger surface area with oxygen-functional groups and π-bonds conjugations. Therefore, protein can be adsorbed on GO through non-covalent including electrostatic, hydrophobic and π-π stacking interactions [242]. In addition, GO side groups and protein could interact through hydrogen bonding which supports the adhesion on the surface, but the hydrophobic interactions remain stronger than electrostatic interactions between GO and protein [242, 243]. Interactions of lipid with GO is unique due to 2D geometry of GO, and it is very important for tissue engineering [244]. A study of single layer interactions to a few layers of GO with bilayers of lipids have been demonstrated with molecular dynamic simulations, and showed a stable form of GO-lipid interactions with smaller perturbations [245]. In addition, another study has pointed out that GO is able to entrench in lipids membrane, and numerous lipids are adsorbed on GO surface and dragged out of the membrane, and thus pores are formed and they allow water molecules to drift into the membrane [246, 247].

6 Clinical potential and major challenges

The unique physicochemical properties of GO including large surface area, chemical purity, high loading capacity of drug due to the double-sided sheet, stability due to oxygen-containing functional groups, and the nature of lipophilic helps in penetration of cell membrane barrier for *in vivo* drug delivery, made GO highly auspicious for anticancer drug delivery nanocarriers [248]. After the work of GO for *in vitro* anticancer drugs loading and release [126], several works of GO-based hydrogel have been published on *in vivo* and *in vitro* loading and release of anticancer drugs. Therefore, it was found that GO, can be easily optimized for their *in vivo* explicit purposes and gain features to be often desired as a carrier in drug delivery system [248, 249]. Additionally, the ability of GO to load aromatic and water-insoluble drug added extra unique features to their clinical potentials, besides their ability to easily pass across the cell membrane [249].

The major challenges for GO-based nanomaterials in anticancer drug delivery applications are to realize (1) the adequate capability of high drug loading for practical usages, (2) the appropriateness of *in vivo* distribution of drug and release profile, (3) the appropriate GO-nanomaterials modifications for penetrating the barrier of cell membrane, and (4) the GO toxicity profile understanding for both *in vivo* and *in vitro*, besides of their biocompatibility, biodistribution and biodegradability. Therefore, the cytotoxicity effects of GO-based nanomaterials should be taken seriously into account in the drug delivery systems, where it is found to be dependent on the particular form of GO such as morphology, chemical structure and size [248, 249].

7 Conclusions and future perspectives

Graphene oxide hydrogels had been extensively examined for biomedical applications, specifically in the anticancer drug delivery system. Graphene oxide physicochemical properties render its higher capacity of anticancer drug loading capacity for hydrophilic and hydrophobic drugs. More importantly, unmodified graphene oxide possesses insignificant toxicity to the normal cell. The modification of graphene oxide with natural or polymers such as chitosan, sodium alginate, carboxymethyl cellulose, polyacrylamide and poly(N-isopropyl acrylamide) improved the mechanical properties, stability and biocompatibility of graphene oxide for delivery of the anticancer drug with well-regulated release profile and non-initial burst. Moreover, some graphene oxide hydrogels accomplished to load multi-drugs such as camptothecin and doxorubicin. In addition, graphene oxide hydrogels could be prepared *via* physical or chemical crosslinking strategy using several crosslinkers such as ester, amide, disulfide, metal ions and azide groups. Natural polymer modified graphene oxide such as chitosan and carboxymethyl cellulose improved the *in vivo* applications. Functionalization of graphene oxide also could be done with stimuli response material such as sodium alginate, a pH-response polymer to trigger drug release upon pH change. Graphene oxide hydrogels could also be engineered to be target cell-specific in order to achieve controlled release anticancer drug. On the other hand, nanoparticles could be incorporated into graphene oxide hydrogels to enhance mechanical properties or add an extra property to the nanocomposites, such as the magnetic property of Fe_3O_4 nanoparticle on graphene oxide. The versatility of graphene oxide hydrogels stimulate more research to be conducted in the biomedical applications, that one would expect to realize its real application in human body in the very near future.

Conflict of interest

The authors confirm that this article content has no conflict of interest.

Acknowledgements

The authors would like to acknowledge the funding from the Ministry of Education Malaysia in the form of FRGS (RDU160118: FRGS/1/2016/STG07/UMP/02/3, RDU170113: FRGS/1/2017/STG07/UMP/01/1), Universiti Malaysia Pahang grant RDU170357 and King Khalid University, the Ministry of Education in Saudi Arabia for supporting this research through grant (RCAMS/KKU/002-18) under research center for advanced material science.

References

[1] Santra, S.; Malhotra, A. Fluorescent nanoparticle probes for imaging of cancer. *Wiley Interdiscip. Rev. Nanomed. Nanobiotechnol.* **2011**, *3*, 501–510.
[2] Ferlay, J.; Soerjomataram, I.; Dikshit, R.; Eser, S.; Mathers, C.; Rebelo, M.; Parkin, D. M.; Forman, D.; Bray, F. Cancer incidence and mortality worldwide: Sources, methods and major patterns in GLOBOCAN 2012. *Int. J. Cancer* **2015**, *136*, E359–E386.
[3] Potash, J.; Anderson, K. C. AACR cancer progress report 2014: Transforming lives through research. *Clin. Cancer Res.* **2014**, *20*, 4977.
[4] Wang, X.; Yang, L.; Chen, Z. G.; Shin, D. M. Application of nanotechnology in cancer therapy and imaging. *CA-Cancer J. Clin.* **2008**, *58*, 97–110.
[5] Ruenraroengsak, P.; Cook, J. M.; Florence, A. T. Nanosystem drug targeting: Facing up to complex realities. *J. Control. Release* **2010**, *141*, 265–276.
[6] Nichols, J. W.; Bae, Y. H. Odyssey of a cancer nanoparticle: From injection site to site of action. *Nano Today* **2012**, *7*, 606–618.
[7] Yezhelyev, M. V.; Gao, X. H.; Xing, Y.; Al-Hajj, A.; Nie, S. M.; O'Regan, R. M. Emerging use of nanoparticles in diagnosis and treatment of breast cancer. *Lancet Oncol.* **2006**, *7*, 657–667.
[8] Haley, B.; Frenkel, E. Nanoparticles for drug delivery in cancer treatment. *Urol. Oncol.* **2008**, *26*, 57–64.
[9] LaVan, D. A.; McGuire, T.; Langer, R. Small-scale systems for *in vivo* drug delivery. *Nat. Biotechnol.* **2003**, *21*, 1184–1191.
[10] Liu, M. J.; Kono, K.; Fréchet, J. M. Water-soluble dendritic unimolecular micelles: Their potential as drug delivery agents. *J. Control. Release* **2000**, *65*, 121–131.
[11] Kim, C. S.; Duncan, B.; Creran, B.; Rotello, V. M. Triggered nanoparticles as therapeutics. *Nano Today* **2013**, *8*, 439–447.
[12] Ge, Z. S.; Liu, S. Y. Functional block copolymer assemblies responsive to tumor and intracellular microenvironments for site-specific drug delivery and enhanced imaging performance. *Chem. Soc. Rev.* **2013**, *42*, 7289–7325.
[13] Issels, R. D. Hyperthermia adds to chemotherapy. *Eur. J. Cancer* **2008**, *44*, 2546–2554.
[14] De La Rica, R.; Aili, D.; Stevens, M. M. Enzyme-responsive nanoparticles for drug release and diagnostics. *Adv. Drug Deliv. Rev.* **2012**, *64*, 967–978.
[15] Gerweck, L. E.; Seetharaman, K. Cellular pH gradient in tumor versus normal tissue: Potential exploitation for the treatment of cancer. *Cancer Res.* **1996**, *56*, 1194–1198.
[16] Deng, C.; Jiang, Y. J.; Cheng, R.; Meng, F. H.; Zhong, Z. Y. Biodegradable polymeric micelles for targeted and controlled anticancer drug delivery: Promises, progress and prospects. *Nano Today* **2012**, *7*, 467–480.
[17] Lee, E. S.; Oh, K. T.; Kim, D.; Youn, Y. S.; Bae, Y. H. Tumor pH-responsive flower-like micelles of poly(L-lactic acid)-*b*-poly(ethylene glycol)-b-poly(L-histidine). *J. Control. Release* **2007**, *123*, 19–26.
[18] Hamidi, M.; Azadi, A.; Rafiei, P. Hydrogel nanoparticles in drug delivery. *Adv. Drug Deliv. Rev.* **2008**, *60*, 1638–1649.
[19] Min, K. H.; Park, K.; Kim, Y.-S.; Bae, S. M.; Lee, S.; Jo, H. G.; Park, R.-W.; Kim, I.-S.; Jeong, S. Y.; Kim, K. et al. Hydrophobically modified glycol chitosan nanoparticles-encapsulated camptothecin enhance the drug stability and tumor targeting in cancer therapy. *J. Control. Release* **2008**, *127*, 208–218.
[20] Vinogradov, S. V.; Bronich, T. K.; Kabanov, A. V. Nanosized cationic hydrogels for drug delivery: Preparation, properties and interactions with cells. *Adv. Drug Deliv. Rev.* **2002**, *54*, 135–147.
[21] Nahar, M.; Dutta, T.; Murugesan, S.; Asthana, A.; Mishra, D.; Rajkumar, V.; Tare, M.; Saraf, S.; Jain, N. K. Functional polymeric nanoparticles: An efficient and promising tool for active delivery of bioactives. *Crit. Rev. Ther. Drug Carrier Syst.* **2006**, *23*, 259–318.
[22] Moghimi, S. M.; Hunter, A. C.; Murray, J. C. Long-circulating and target-specific nanoparticles: Theory to practice. *Pharmacol. Rev.* **2001**, *53*, 283–318.
[23] Peppas, N. A.; Mikos, A. G. Preparation methods and structure of hydrogels. In *Hydrogels in Medicine and Pharmacy*. Peppas, N., Ed.; CRC Press: Boca Raton, FL, 1986; pp 1–27.
[24] Brannon-Peppas, L. Preparation and characterization of crosslinked hydrophilic networks. In *Adsorbent Polymer Technology*. Brannon-Peppas, L.; Harland, R. S., Eds.; Elsevier: Amsterdam, 1990; pp 45–66.
[25] Peppas, N. A.; Khare, A. R. Preparation, structure and diffusional behavior of hydrogels in controlled release. *Adv. Drug Deliv. Rev.* **1993**, *11*, 1–35.
[26] Hacker, M.; Mikos, A. Synthetic polymers. In *Principles of Regenerative Medicine*. Atala, A.; Lanza, R.; Thomson, J. A.; Nerem, R. M., Eds.; Academic press; San Diego, 2011; pp 587–622.
[27] Das, N. Preparation methods and properties of hydrogel: A review. *Int. J. Pharm. Pharm. Sci.* **2013**, *5*, 112–117.
[28] Goenka, S.; Sant, V.; Sant, S. Graphene-based nanomaterials for drug delivery and tissue engineering. *J. Control. Release* **2014**, *173*, 75–88.
[29] Novoselov, K. S.; Fal'ko, V. I.; Colombo, L.; Gellert, P. R.; Schwab, M. G.; Kim, K. A roadmap for graphene. *Nature* **2012**, *490*, 192–200.
[30] Ali, G. A. M.; Makhlouf, S. A.; Yusoff, M. M.; Chong, K. F. Structural and electrochemical characteristics of graphene nanosheets as supercapacitor electrodes. *Rev. Adv. Mater. Sci.* **2015**, *41*, 35–43.
[31] Allen, M. J.; Tung, V. C.; Kaner, R. B. Honeycomb carbon: A review of graphene. *Chem. Rev.* **2010**, *110*, 132–145.
[32] Geim, A. K. Graphene: Status and prospects. *Science* **2009**, *324*, 1530–1534.
[33] Wang, Y.; Li, Z. H.; Wang, J.; Li, J. H.; Lin, Y. H. Graphene and graphene oxide: Biofunctionalization and applications in biotechnology. *Trends Biotechnol.* **2011**, *29*, 205–212.
[34] Butler, S. Z.; Hollen, S. M.; Cao, L. Y.; Cui, Y.; Gupta, J. A.; Gutiérrez, H. R.; Heinz, T. F.; Hong, S. S.; Huang, J. X.; Ismach, A. F. et al. Progress, challenges, and opportunities in two-dimensional materials beyond graphene. *ACS Nano* **2013**, *7*, 2898–2926.
[35] Huang, P.; Xu, C.; Lin, J.; Wang, C.; Wang, X. S.; Zhang, C. L.; Zhou, X. J.; Guo, S. W.; Cui, D. X. Folic acid-conjugated graphene oxide loaded with photosensitizers for targeting photodynamic therapy. *Theranostics* **2011**, *1*, 240–250.
[36] Zhang, J. L.; Yang, H. J.; Shen, G. X.; Cheng, P.; Zhang, J. Y.; Guo, S. W. Reduction of graphene oxide via *L*-ascorbic acid. *Chem. Commun.* **2010**, *46*, 1112–1114.
[37] Zhang, J. L.; Zhang, F.; Yang, H. J.; Huang, X. L.; Liu, H.; Zhang, J. Y.; Guo, S. W. Graphene oxide as a matrix for enzyme immobilization. *Langmuir* **2010**, *26*, 6083–6085.
[38] Haubner, K.; Murawski, J.; Olk, P.; Eng, L. M.; Ziegler, C.; Adolphi, B.; Jaehne, E. The route to functional graphene oxide. *ChemPhysChem* **2010**, *11*, 2131–2139.
[39] Nurunnabi, M.; Parvez, K.; Nafiujjaman, M.; Revuri, V.; Khan, H. A.; Feng, X. L.; Lee, Y.-K. Bioapplication of graphene oxide derivatives: Drug/gene delivery, imaging, polymeric modification, toxicology, therapeutics and challenges. *RSC Adv.* **2015**, *5*, 42141–42161.
[40] Yang, K.; Wan, J.; Zhang, S.; Zhang, Y.; Lee, S.-T.; Liu, Z. *In vivo* pharmacokinetics, long-term biodistribution, and toxicology of PEGylated graphene in mice. *ACS Nano* **2011**, *5*, 516–522.
[41] Wang, C. Y.; Wang, X. Q.; Lu, T.; Liu, F. S.; Guo, B. F.; Wen, N. Y.; Du, Y. W.; Lin, H.; Tang, J.; Zhang, L. Multi-functionalized graphene oxide complex as a plasmid delivery system for targeting hepatocellular carcinoma therapy. *RSC Adv.* **2016**, *6*, 22461–22468.
[42] Li, H.; Luo, R. M.; Lam, K. Y. Modeling of environmentally sensitive hydrogels for drug delivery: An overview and recent developments. *Front. Drug Des. Discov.* **2006**, *2*, 295–331.
[43] Ahmed, E. M. Hydrogel: Preparation, characterization, and applications: A review. *J. Adv. Res.* **2015**, *6*, 105–121.
[44] Cha, C.; Shin, S. R.; Gao, X. G.; Annabi, N.; Dokmeci, M. R.; Tang, X. S.; Khademhosseini, A. Controlling mechanical properties of cell-laden hydrogels by covalent incorporation of graphene oxide. *Small* **2014**, *10*, 514–523.
[45] Holloway, J. L.; Ma, H.; Rai, R.; Burdick, J. A. Modulating hydrogel crosslink density and degradation to control bone morphogenetic protein delivery and *in vivo* bone formation. *J. Control. Release* **2014**, *191*, 63–70.
[46] Lee, S. C.; Kwon, I. K.; Park, K. Hydrogels for delivery of bioactive agents: A historical perspective. *Adv. Drug Deliv. Rev.* **2013**, *65*, 17–20.
[47] Wichterle, O.; Lím, D. Hydrophilic gels for biological use. *Nature* **1960**, *185*, 117–118.
[48] Buwalda, S. J.; Boere, K. W. M.; Dijkstra, P. J.; Feijen, J.; Vermonden, T.; Hennink, W. E. Hydrogels in a historical perspective: From simple networks to smart materials. *J. Control. Release* **2014**, *190*, 254–273.

[49] Sharma, K.; Kumar, V.; Kaith, B. S.; Kalia, S.; Swart, H. C. Conducting polymer hydrogels and their applications. In *Conducting Polymer Hybrids*. Kumar; V.; Kalia, S.; Swart, H. C., Eds.; Springer: Switzerland, 2017; pp 193–221.
[50] Haque, M. A.; Kurokawa, T.; Gong, J. P. Super tough double network hydrogels and their application as biomaterials. *Polymer* **2012**, *53*, 1805–1822.
[51] Varaprasad, K.; Raghavendra, G. M.; Jayaramudu, T.; Yallapu, M. M.; Sadiku, R. A mini review on hydrogels classification and recent developments in miscellaneous applications. *Mater. Sci. Eng. C* **2017**, *79*, 958–971.
[52] Akhtar, M. F.; Hanif, M.; Ranjha, N. M. Methods of synthesis of hydrogels… A review. *Saudi Pharm. J.* **2016**, *24*, 554–559.
[53] Zu, Y. G.; Zhang, Y.; Zhao, X. H.; Shan, C.; Zu, S. C.; Wang, K. L.; Li, Y.; Ge, Y. L. Preparation and characterization of chitosan–polyvinyl alcohol blend hydrogels for the controlled release of nano-insulin. *Int. J. Biol. Macromol.* **2012**, *50*, 82–87.
[54] Lugao, A. B.; Malmonge, S. M. Use of radiation in the production of hydrogels. *Nucl. Instrum. Meth. Phys. Res. B* **2001**, *185*, 37–42.
[55] Sperinde, J. J.; Griffith, L. G. Synthesis and characterization of enzymatically-cross-linked poly(ethylene glycol) hydrogels. *Macromolecules* **1997**, *30*, 5255–5264.
[56] Ullah, F.; Othman, M. B. H.; Javed, F.; Ahmad, Z.; Akil, H. M. Classification, processing and application of hydrogels: A review. *Mater. Sci. Eng. C* **2015**, *57*, 414–433.
[57] Daoud Attieh, M.; Zhao, Y.; Elkak, A.; Falcimaigne-Cordin, A.; Haupt, K. Enzyme-initiated free-radical polymerization of molecularly imprinted polymer nanogels on a solid phase with an immobilized radical source. *Angew. Chem., Int. Ed.* **2017**, *56*, 3339–3343.
[58] Chen, Q.; Zhu, L.; Zhao, C.; Wang, Q. M.; Zheng, J. A robust, one-pot synthesis of highly mechanical and recoverable double network hydrogels using thermoreversible sol-gel polysaccharide. *Adv. Mater.* **2013**, *25*, 4171–4176.
[59] Zhang, L.; Zheng, G.-J.; Guo, Y.-T.; Zhou, L.; Du, J.; He, H. Preparation of novel biodegradable pHEMA hydrogel for a tissue engineering scaffold by microwave-assisted polymerization. *Asian Pac. J. Trop. Med.* **2014**, *7*, 136–140.
[60] Atzet, S.; Curtin, S.; Trinh, P.; Bryant, S.; Ratner, B. Degradable poly(2-hydroxyethyl methacrylate)-*co*-polycaprolactone hydrogels for tissue engineering scaffolds. *Biomacromolecules* **2008**, *9*, 3370–3377.
[61] Sharma, R.; Kalia, S.; Kaith, B. S.; Kumar, A.; Thakur, P.; Pathania, D.; Srivastava, M. K. Ggum-poly(itaconic acid) based superabsorbents via two-step free-radical aqueous polymerization for environmental and antibacterial applications. *J. Polym. Environ.* **2017**, *25*, 176–191.
[62] Sarika, P. R.; Cinthya, K.; Jayakrishnan, A.; Anilkumar, P. R.; James, N. R. Modified gum arabic cross-linked gelatin scaffold for biomedical applications. *Mater. Sci. Eng. C* **2014**, *43*, 272–279.
[63] Coviello, T.; Grassi, M.; Rambone, G.; Santucci, E.; Carafa, M.; Murtas, E.; Riccieri, F. M.; Alhaique, F. Novel hydrogel system from scleroglucan: Synthesis and characterization. *J. Control. Release* **1999**, *60*, 367–378.
[64] Chung, T.-W.; Chou, T.-H.; Wu, K.-Y. Gelatin/PLGA hydrogel films and their delivery of hydrophobic drugs. *J. Taiwan Inst. Chem. E.* **2016**, *60*, 8–14.
[65] Chen, Y.-Y.; Wu, H.-C.; Sun, J.-S.; Dong, G.-C.; Wang, T.-W. Injectable and thermoresponsive self-assembled nanocomposite hydrogel for long-term anticancer drug delivery. *Langmuir* **2013**, *29*, 3721–3729.
[66] Yoshimura, T.; Hirao, N.; Fujioka, R. Preparation and characterization of biodegradable hydrogels based on ulvan, a polysaccharide from green seaweeds. *Polym. Renew. Resour.* **2016**, *7*, 33–41.
[67] Riahi, N.; Liberelle, B.; Henry, O.; De Crescenzo, G. Impact of RGD amount in dextran-based hydrogels for cell delivery. *Carbohyd. Polym.* **2017**, *161*, 219–227.
[68] Noteborn, W. E. M.; Gao, Y.; Jesse, W.; Kros, A.; Kieltyka, R. E. Dual-crosslinked human serum albumin-polymer hydrogels for affinity-based drug delivery. *Macromol. Mater. Eng.* **2017**, *302*, 1700243.
[69] Kuijpers, A. J.; Van Wachem, P. B.; Van Luyn, M. J.; Engbers, G. H. M.; Krijgsveld, J.; Zaat, S. A. J.; Dankert, J.; Feijen, J. *In vivo* and *in vitro* release of lysozyme from cross-linked gelatin hydrogels: A model system for the delivery of antibacterial proteins from prosthetic heart valves. *J. Control. Release* **2000**, *67*, 323–336.
[70] Omobono, M. A.; Zhao, X.; Furlong, M. A.; Kwon, C. H.; Gill, T. J.; Randolph, M. A.; Redmond, R. W. Enhancing the stiffness of collagen hydrogels for delivery of encapsulated chondrocytes to articular lesions for cartilage regeneration. *J. Biomed. Mater. Res. A* **2015**, *103*, 1332–1338.
[71] Ghorpade, V. S.; Yadav, A. V.; Dias, R. J. Citric acid crosslinked cyclodextrin/hydroxypropylmethylcellulose hydrogel films for hydrophobic drug delivery. *Int. J. Biol. Macromol.* **2016**, *93*, 75–86.
[72] Seki, Y.; Altinisik, A.; Demircioğlu, B.; Tetik, C. Carboxymethylcellulose (CMC)–hydroxyethylcellulose (HEC) based hydrogels: Synthesis and characterization. *Cellulose* **2014**, *21*, 1689–1698.
[73] Gupta, A. P.; Arora, G. Preparation and characterization of guar-gum/polyvinylalcohol blend films. *J. Mater. Sci. Eng. B* **2011**, *1*, 28–33.
[74] Rudick, J. G. Innovative macromolecular syntheses via isocyanide multicomponent reactions. *J. Polym. Sci. A: Polym. Chem.* **2013**, *51*, 3985–3991.
[75] De Nooy, A. E.; Capitani, D.; Masci, G.; Crescenzi, V. Ionic polysaccharide hydrogels via the Passerini and Ugi multicomponent condensations: Synthesis, behavior and solid-state NMR characterization. *Biomacromolecules* **2000**, *1*, 259–267.
[76] El-Gendy, A. A.; Abou-Yousef, H.; Adel, A.; El-Shinnawy, N. Bio-based hydrogel formed by gamma irradiation. *Egypt. J. Chem.* **2016**, *59*, 647–662.
[77] Tohfafarosh, M.; Baykal, D.; Kiel, J. W.; Mansmann, K.; Kurtz, S. M. Effects of gamma and e-beam sterilization on the chemical, mechanical and tribological properties of a novel hydrogel. *J. Mech. Behav. Biomed. Mater.* **2016**, *53*, 250–256.
[78] Wach, R. A.; Rokita, B.; Bartoszek, N.; Katsumura, Y.; Ulanski, P.; Rosiak, J. M. Hydroxyl radical-induced crosslinking and radiation-initiated hydrogel formation in dilute aqueous solutions of carboxymethylcellulose. *Carbohyd. Polym.* **2014**, *112*, 412–415.
[79] Fekete, T.; Borsa, J.; Takács, E.; Wojnárovits, L. Synthesis of cellulose derivative based superabsorbent hydrogels by radiation induced crosslinking. *Cellulose* **2014**, *21*, 4157–4165.
[80] Park, J.-S.; Kuang, J.; Gwon, H.-J.; Lim, Y.-M.; Jeong, S.-I.; Shin, Y.-M.; Khil, M. S.; Nho, Y.-C. Synthesis and characterization of zinc chloride containing poly(acrylic acid) hydrogel by gamma irradiation. *Radiat. Phys. Chem.* **2013**, *88*, 60–64.
[81] Yamdej, R.; Pangza, K.; Srichana, T.; Aramwit, P. Superior physicochemical and biological properties of poly(vinyl alcohol)/sericin hydrogels fabricated by a non-toxic gamma-irradiation technique. *J. Bioact. Compat. Polym.* **2017**, *32*, 32–44.
[82] Banaei, M.; Dehshiri, S.; Shirmardi, S. P. Physical Swelling Properties study of a PVP hydrogel in aqueous solutions by using electron beam (EB) irradiation. *J. Nucl. Ene. Sci. Power Generat. Technol.* **2016**, *5*, DOI: 10.4172/2325-9809.1000147.
[83] Fekete, T.; Borsa, J.; Takács, E.; Wojnárovits, L. Synthesis of carboxymethylcellulose/starch superabsorbent hydrogels by gamma-irradiation. *Chem. Cent. J.* **2017**, *11*, 46.
[84] Elbarbary, A. M.; Ghobashy, M. M. Phosphorylation of chitosan/HEMA interpenetrating polymer network prepared by γ-radiation for metal ions removal from aqueous solutions. *Carbohyd. Polym.* **2017**, *162*, 16–27.
[85] Sperinde, J. J.; Griffith, L. G. Control and prediction of gelation kinetics in enzymatically cross-linked poly(ethylene glycol) hydrogels. *Macromolecules* **2000**, *33*, 5476–5480.
[86] Arora, A.; Mahajan, A.; Katti, D. S. TGF-β1 presenting enzymatically cross-linked injectable hydrogels for improved chondrogenesis. *Colloids Surf. B: Biointerfaces* **2017**, *159*, 838–848.
[87] Broguiere, N.; Isenmann, L.; Zenobi-Wong, M. Novel enzymatically cross-linked hyaluronan hydrogels support the formation of 3D neuronal networks. *Biomaterials* **2016**, *99*, 47–55.
[88] Wu, C. Z.; Strehmel, C.; Achazi, K.; Chiappisi, L.; Dernedde, J.; Lensen, M. C.; Gradzielski, M.; Ansorge-Schumacher, M. B.; Haag, R. Enzymatically cross-linked hyperbranched polyglycerol hydrogels as scaffolds for living cells. *Biomacromolecules* **2014**, *15*, 3881–3890.
[89] Da Silva, M. A.; Bode, F.; Grillo, I.; Dreiss, C. A. Exploring the kinetics of gelation and final architecture of enzymatically cross-linked chitosan/gelatin gels. *Biomacromolecules* **2015**, *16*, 1401–1409.
[90] Le Thi, P.; Lee, Y.; Nguyen, D. H.; Park, K. D. *In situ* forming gelatin hydrogels by dual-enzymatic cross-linking for enhanced tissue adhesiveness. *J. Mater. Chem. B* **2017**, *5*, 757–764.
[91] Gulrez, S. K. H.; Al-Assaf, S.; Phillips, G. O. Hydrogels: Methods of preparation, characterisation and applications. In *Progress in Molecular and Environmental Bioengineering*. Carpi, A., Ed.; InTech: UK, 2011; pp 117–150.
[92] Gyles, D. A.; Castro, L. D.; Silva, J. O. C., Jr.; Ribeiro-Costa, R. M. A review of the designs and Prominent Biomedical Advances of Natural and

Synthetic Hydrogel Formulations. *Eur. Polym. J.* **2017**, *88*, 373–392.
[93] Agrawal, G.; Pich, A. Polymer gels as EAPs: Materials. In *Electromechanically Active Polymers*. Carpi, F., Ed.; Springer International Publishing: Switzerland, 2016; pp 1–27.
[94] Hennink, W. E.; Van Nostrum, C. F. Novel crosslinking methods to design hydrogels. *Adv. Drug Deliv. Rev.* **2012**, *64*, 223–236.
[95] Yang, C. H.; Wang, M. X.; Haider, H.; Yang, J. H.; Sun, J.-Y.; Chen, Y. M.; Zhou, J. X.; Suo, Z. G. Strengthening alginate/polyacrylamide hydrogels using various multivalent cations. *ACS Appl. Mater. Interfaces* **2013**, *5*, 10418–10422.
[96] Girgin, B.; Korkmaz, O.; Yavaşer, R.; Karagözler, A. A. Production and drug release assesment of melatonin-loaded alginate/gum arabic beads. *J. Turkish Chem. Soc. Sect. A: Chem.* **2016**, *3*, 205–216.
[97] Rezvanain, M.; Ahmad, N.; Amin, M. C. I. M.; Ng, S.-F. Optimization, characterization, and *in vitro* assessment of alginate-pectin ionic cross-linked hydrogel film for wound dressing applications. *Int. J. Biol. Macromol.* **2017**, *97*, 131–140.
[98] Li, G.; Zhang, G. P.; Sun, R.; Wong, C.-P. Mechanical strengthened alginate/polyacrylamide hydrogel crosslinked by barium and ferric dual ions. *J. Mater. Sci.* **2017**, *52*, 8538–8545.
[99] Hirschberg, J. H. K. K.; Brunsveld, L.; Ramzi, A.; Vekemans, J. A. J. M.; Sijbesma, R. P.; Meijer, E. W. Helical self-assembled polymers from cooperative stacking of hydrogen-bonded pairs. *Nature* **2000**, *407*, 167–170.
[100] Li, G.; Yan, Q.; Xia, H. S.; Zhao, Y. Therapeutic-ultrasound-triggered shape memory of a melamine-enhanced poly(vinyl alcohol) physical hydrogel. *ACS Appl. Mater. Interfaces* **2015**, *7*, 12067–12073.
[101] Shi, S. J.; Peng, X.; Liu, T. Q.; Chen, Y.-N.; He, C. C.; Wang, H. L. Facile preparation of hydrogen-bonded supramolecular polyvinyl alcohol-glycerol gels with excellent thermoplasticity and mechanical properties. *Polymer* **2017**, *111*, 168–176.
[102] Li, G.; Zhang, H. J.; Fortin, D.; Xia, H. S.; Zhao, Y. Poly (vinyl alcohol)–Poly(ethylene glycol) double-network hydrogel: A general approach to shape memory and self-healing functionalities. *Langmuir* **2015**, *31*, 11709–11716.
[103] Li, J. F.; Wang, Z. L.; Wen, L. G.; Nie, J.; Yang, S. G.; Xu, J.; Cheng, S. Z. D. Highly elastic fibers made from hydrogen-bonded polymer complex. *ACS Macro Lett.* **2016**, *5*, 814–818.
[104] Dai, X. Y.; Zhang, Y. Y.; Gao, L.; Bai, T.; Wang, W.; Cui, Y. L.; Liu, W. G. A Mechanically strong, highly stable, thermoplastic, and self-healable supramolecular polymer hydrogel. *Adv. Mater.* **2015**, *27*, 3566–3571.
[105] Hassan, C. M.; Peppas, N. A. Structure and applications of poly(vinyl alcohol) hydrogels produced by conventional crosslinking or by freezing/thawing methods. In *Biopolymers· PVA Hydrogels, Anionic Polymerisation Nanocomposites. Advances in Polymer Science*. Springer: Berlin, 2000; pp 37–65.
[106] Förster, S.; Antonietti, M. Amphiphilic block copolymers in structure-controlled nanomaterial hybrids. *Adv. Mater.* **1998**, *10*, 195–217.
[107] Lee, D. S.; Jeong, B.; Bae, Y. H.; Kim, S. W. New thermoreversible and biodegradable block copolymer hydrogels. *Proc. Control. Release Soc.* **1996**, (23), 228–229.
[108] Jeong, B.; Bae, Y. H.; Kim, S. W. Thermoreversible gelation of PEG-PLGA-PEG triblock copolymer aqueous solutions. *Macromolecules* **1999**, *32*, 7064–7069.
[109] Buwalda, S. J.; Nottelet, B.; Coudane, J. Robust & thermosensitive poly(ethylene glycol)-poly(ε-caprolactone) star block copolymer hydrogels. *Polym. Degrad. Stabil.* **2017**, *137*, 173–183.
[110] Hom, W. L.; Bhatia, S. R. Significant enhancement of elasticity in alginate-clay nanocomposite hydrogels with PEO-PPO-PEO copolymers. *Polymer* **2017**, *109*, 170–175.
[111] Cappello, J.; Crissman, J.; Dorman, M.; Mikolajczak, M.; Textor, G.; Marquet, M.; Ferrari, F. Genetic engineering of structural protein polymers. *Biotechnol. Progr.* **1990**, *6*, 198–202.
[112] McGrath, K. P.; Fournier, M. J.; Mason, T. L.; Tirrell, D. A. Genetically directed syntheses of new polymeric materials. Expression of artificial genes encoding proteins with repeating-(AlaGly) 3ProGluGly-elements. *J. Am. Chem. Soc.* **1992**, *114*, 727–733.
[113] Vagias, A.; Sergelen, K.; Koynov, K.; Košovan, P.; Dostalek, J.; Jonas, U.; Knoll, W.; Fytas, G. Diffusion and permeation of labeled IgG in grafted hydrogels. *Macromolecules* **2017**, *50*, 4770–4779.
[114] Li, H. B.; Kong, N.; Laver, B.; Liu, J. Q. Hydrogels constructed from engineered proteins. *Small* **2016**, *12*, 973–987.
[115] Yang, W. Z.; Wang, M. M.; Ma, L. L.; Li, H. Y.; Huang, L. Synthesis and characterization of biotin modified cholesteryl pullulan as a novel anticancer drug carrier. *Carbohyd. Polym.* **2014**, *99*, 720–727.
[116] Xin, C.; Chen, J.; Liang, H. S.; Wan, J. W.; Li, J.; Li, B. Confirmation and measurement of hydrophobic interaction in sol-gel system of konjac glucomannan with different degree of deacetylation. *Carbohyd. Polym.* **2017**, *174*, 337–342.
[117] Becerra, J.; Sudre, G.; Royaud, I.; Montserret, R.; Verrier, B.; Rochas, C.; Delair, T.; David, L. Tuning the hydrophilic/hydrophobic balance to control the structure of chitosan films and their protein release behavior. *AAPS PharmSciTech* **2017**, *18*, 1070–1083.
[118] Bai, H.; Li, C.; Shi, G. Q. Functional composite materials based on chemically converted graphene. *Adv. Mater.* **2011**, *23*, 1089–1115.
[119] Schniepp, H. C.; Li, J.-L.; McAllister, M. J.; Sai, H.; Herrera-Alonso, M.; Adamson, D. H.; Prud'homme, R. K.; Car, R.; Saville, D. A.; Aksay, I. A. Functionalized single graphene sheets derived from splitting graphite oxide. *J. Phys. Chem. B* **2006**, *110*, 8535–8539.
[120] Hummers, W. S., Jr.; Offeman, R. E. Preparation of graphitic oxide. *J. Am. Chem. Soc.* **1958**, *80*, 1339.
[121] Lerf, A.; He, H. Y.; Forster, M.; Klinowski, J. Structure of graphite oxide revisited. *J. Phys. Chem. B* **1998**, *102*, 4477–4482.
[122] Nasrollahzadeh, M.; Babaei, F.; Fakhri, P.; Jaleh, B. Synthesis, characterization, structural, optical properties and catalytic activity of reduced graphene oxide/copper nanocomposites. *RSC Adv.* **2015**, *5*, 10782–10789.
[123] Zhang, Q.; Wu, Z. N.; Li, N.; Pu, Y. Q.; Wang, B.; Zhang, T.; Tao, J. S. Advanced review of graphene-based nanomaterials in drug delivery systems: Synthesis, modification, toxicity and application. *Mater. Sci. Eng. C* **2017**, *77*, 1363–1375.
[124] Travlou, N. A.; Kyzas, G. Z.; Lazaridis, N. K.; Deliyanni, E. A. Functionalization of graphite oxide with magnetic chitosan for the preparation of a nanocomposite dye adsorbent. *Langmuir* **2013**, *29*, 1657–1668.
[125] Sun, X. M.; Liu, Z.; Welsher, K.; Robinson, J. T.; Goodwin, A.; Zaric, S.; Dai, H. J. Nano-graphene oxide for cellular imaging and drug delivery. *Nano Res.* **2008**, *1*, 203–212.
[126] Liu, Z.; Robinson, J. T.; Sun, X. M.; Dai, H. J. PEGylated nanographene oxide for delivery of water-insoluble cancer drugs. *J. Am. Chem. Soc.* **2008**, *130*, 10876–10877.
[127] Chen, L.; Zhong, X. Y.; Yi, X.; Huang, M.; Ning, P.; Liu, T.; Ge, C. C.; Chai, Z. F.; Liu, Z.; Yang, K. Radionuclide ^{131}I labeled reduced graphene oxide for nuclear imaging guided combined radio- and photothermal therapy of cancer. *Biomaterials* **2015**, *66*, 21–28.
[128] Jiang, B.; Qu, Y. Y.; Zhang, L. H.; Liang, Z.; Zhang, Y. K. 4-Mercapto-phenylboronic acid functionalized graphene oxide composites: Preparation, characterization and selective enrichment of glycopeptides. *Anal. Chim. Acta* **2016**, *912*, 41–48.
[129] Hu, H. Q.; Yu, J. H.; Li, Y. Y.; Zhao, J.; Dong, H. Q. Engineering of a novel pluronic F127/graphene nanohybrid for pH responsive drug delivery. *J. Biomed. Mater. Res. A* **2012**, *100*, 141–148.
[130] Liu, S. L.; Ling, J.; Li, K. W.; Yao, F.; Oderinde, O.; Zhang, Z. H.; Fu, G. D. Bio-inspired and lanthanide-induced hierarchical sodium alginate/graphene oxide composite paper with enhanced physicochemical properties. *Compos. Sci. Technol.* **2017**, *145*, 62–70.
[131] Peng, X.; He, C. C.; Liu, J. Q.; Wang, H. L. Biomimetic jellyfish-like PVA/graphene oxide nanocomposite hydrogels with anisotropic and pH-responsive mechanical properties. *J. Mater. Sci.* **2016**, *51*, 5901–5911.
[132] Stankovich, S.; Piner, R. D.; Chen, X. Q.; Wu, N. Q.; Nguyen, S. T.; Ruoff, R. S. Stable aqueous dispersions of graphitic nanoplatelets via the reduction of exfoliated graphite oxide in the presence of poly(sodium 4-styrenesulfonate). *J. Mater. Chem.* **2006**, *16*, 155–158.
[133] Yang, Y.; Zhang, Y. M.; Chen, Y.; Zhao, D.; Chen, J. T.; Liu, Y. Construction of a graphene oxide based noncovalent multiple nanosupramolecular assembly as a scaffold for drug delivery. *Chem.—Eur. J* **2012**, *18*, 4208–4215.
[134] Wang, J.; Chen, Z. M.; Chen, B. L. Adsorption of polycyclic aromatic hydrocarbons by graphene and graphene oxide nanosheets. *Environ. Sci. Technol.* **2014**, *48*, 4817–4825.
[135] Azadbakht, A.; Roushani, M.; Abbasi, A. R.; Derikvand, Z.; Menati, S. Bifunctional impedimetric sensors based on azodicarboxamide supported on modified graphene nanosheets. *Mater. Sci. Eng. C* **2016**, *69*, 221–230.
[136] Yu, Y.; Shu, Y.; Ye, L. *In situ* crosslinking of poly (vinyl alcohol)/graphene oxide-glutamic acid nano-composite hydrogel as microbial carrier: Intercalation structure and its wastewater treatment performance.

Chem.—Eng. J. **2018**, *336*, 306–314.
[137] Park, Y. H.; Park, S. Y.; In, I. Direct noncovalent conjugation of folic acid on reduced graphene oxide as anticancer drug carrier. *J. Ind. Eng. Chem.* **2015**, *30*, 190–196.
[138] Hu, X. G.; Zhou, Q. X. Health and ecosystem risks of graphene. *Chem. Rev.* **2013**, *113*, 3815–3835.
[139] Seabra, A. B.; Paula, A. J.; de Lima, R.; Alves, O. L.; Durán, N. Nanotoxicity of graphene and graphene oxide. *Chem. Res. Toxicol.* **2014**, *27*, 159–168.
[140] Zhao, J.; Wang, Z. Y.; White, J. C.; Xing, B. S. Graphene in the aquatic environment: Adsorption, dispersion, toxicity and transformation. *Environ. Sci. Technol.* **2014**, *48*, 9995–10009.
[141] Tonelli, F. M.; Goulart, V. A.; Gomes, K. N.; Ladeira, M. S.; Santos, A. K.; Lorençon, E.; Ladeira, L. O.; Resende, R. R. Graphene-based nanomaterials: Biological and medical applications and toxicity. *Nanomedicine* **2015**, *10*, 2423–2450.
[142] Bitounis, D.; Ali-Boucetta, H.; Hong, B. H.; Min, D. H.; Kostarelos, K. Prospects and challenges of graphene in biomedical applications. *Adv. Mater.* **2013**, *25*, 2258–2268.
[143] Bianco, A. Graphene: Safe or toxic? The two faces of the medal. *Angew. Chem., Int. Ed.* **2013**, *52*, 4986–4997.
[144] Yang, K.; Li, Y. J.; Tan, X. F.; Peng, R.; Liu, Z. Behavior and toxicity of graphene and its functionalized derivatives in biological systems. *Small* **2013**, *9*, 1492–1503.
[145] Sanchez, V. C.; Jachak, A.; Hurt, R. H.; Kane, A. B. Biological interactions of graphene-family nanomaterials: An interdisciplinary review. *Chem. Res. Toxicol.* **2012**, *25*, 15–34.
[146] Jastrzębska, A. M.; Kurtycz, P.; Olszyna, A. R. Recent advances in graphene family materials toxicity investigations. *J. Nanopart. Res.* **2012**, *14*, 1320.
[147] Zhang, B. M.; Wang, Y.; Zhai, G. X. Biomedical applications of the graphene-based materials. *Mater. Sci. Eng. C* **2016**, *61*, 953–964.
[148] Wong, C. H. A.; Sofer, Z.; Kubešová, M.; Kučera, J.; Matějková, S.; Pumera, M. Synthetic routes contaminate graphene materials with a whole spectrum of unanticipated metallic elements. *Proc. Natl. Acad. Sci. USA* **2014**, *111*, 13774–13779.
[149] Ambrosi, A.; Chua, C. K.; Khezri, B.; Sofer, Z.; Webster, R. D.; Pumera, M. Chemically reduced graphene contains inherent metallic impurities present in parent natural and synthetic graphite. *Proc. Natl. Acad. Sci. USA* **2012**, *109*, 12899–12904.
[150] Mullick Chowdhury, S.; Dasgupta, S.; McElroy, A. E.; Sitharaman, B. Structural disruption increases toxicity of graphene nanoribbons. *J. Appl. Toxicol.* **2014**, *34*, 1235–1246.
[151] Zhang, Y. B.; Ali, S. F.; Dervishi, E.; Xu, Y.; Li, Z. R.; Casciano, D.; Biris, A. S. Cytotoxicity effects of graphene and single-wall carbon nanotubes in neural phaeochromocytoma-derived PC12 cells. *ACS Nano* **2010**, *4*, 3181–3186.
[152] Vallabani, N. V.; Mittal, S.; Shukla, R. K.; Pandey, A. K.; Dhakate, S. R.; Pasricha, R.; Dhawan, A. Toxicity of graphene in normal human lung cells (BEAS-2B). *J. Biomed. Nanotechnol.* **2011**, *7*, 106–107.
[153] Sasidharan, A.; Panchakarla, L. S.; Chandran, P.; Menon, D.; Nair, S.; Rao, C. N. R.; Koyakutty, M. Differential nano-bio interactions and toxicity effects of pristine versus functionalized graphene. *Nanoscale* **2011**, *3*, 2461–2464.
[154] Horváth, L.; Magrez, A.; Burghard, M.; Kern, K.; Forró, L.; Schwaller, B. Evaluation of the toxicity of graphene derivatives on cells of the lung luminal surface. *Carbon* **2013**, *64*, 45–60.
[155] Akhavan, O.; Ghaderi, E.; Akhavan, A. Size-dependent genotoxicity of graphene nanoplatelets in human stem cells. *Biomaterials* **2012**, *33*, 8017–8025.
[156] Muthoosamy, K.; Bai, R. G.; Manickam, S. Graphene and graphene oxide as a docking station for modern drug delivery system. *Curr. Drug Deliv.* **2014**, *11*, 701–718.
[157] Yang, K.; Feng, L. Z.; Shi, X. Z.; Liu, Z. Nano-graphene in biomedicine: Theranostic applications. *Chem. Soc. Rev.* **2013**, *42*, 530–547.
[158] Yang, X. Y.; Zhang, X. Y.; Liu, Z. F.; Ma, Y. F.; Huang, Y.; Chen, Y. S. High-efficiency loading and controlled release of doxorubicin hydrochloride on graphene oxide. *J. Phys. Chem. C* **2008**, *112*, 17554–17558.
[159] Ni, Y. N.; Zhang, F. Y.; Kokot, S. Graphene oxide as a nanocarrier for loading and delivery of medicinal drugs and as a biosensor for detection of serum albumin. *Anal. Chim. Acta* **2013**, *769*, 40–48.
[160] Wang, Z. H.; Gao, Y. L.; Xia, J. F.; Zhang, F. F.; Xia, Y. Z.; Li, Y. H. Synthesis and characterization of glycyrrhizin-decorated graphene oxide for hepatocyte-targeted delivery. *C. R. Chim.* **2012**, *15*, 708–713.
[161] Zhang, Q.; Li, W. W.; Kong, T.; Su, R. G.; Li, N.; Song, Q.; Tang, M. L.; Liu, L. W.; Cheng, G. S. Tailoring the interlayer interaction between doxorubicin-loaded graphene oxide nanosheets by controlling the drug content. *Carbon* **2013**, *51*, 164–172.
[162] Ma, D.; Lin, J. T.; Chen, Y. Y.; Xue, W.; Zhang, L.-M. *In situ* gelation and sustained release of an antitumor drug by graphene oxide nanosheets. *Carbon* **2012**, *50*, 3001–3007.
[163] Zhou, L.; Zhou, L.; Wei, S. H.; Ge, X. F.; Zhou, J. H.; Jiang, H. J.; Li, F. Y.; Shen, J. Combination of chemotherapy and photodynamic therapy using graphene oxide as drug delivery system. *J. Photochem. Photobiol. B* **2014**, *135*, 7–16.
[164] Zhou, L.; Wang, W.; Tang, J.; Zhou, J. H.; Jiang, H. J.; Shen, J. Graphene oxide noncovalent photosensitizer and its anticancer activity *in vitro*. *Chem.—Eur. J.* **2011**, *17*, 12084–12091.
[165] Hasanzade, Z.; Raissi, H. Solvent/co-solvent effects on the electronic properties and adsorption mechanism of anticancer drug thioguanine on graphene oxide surface as a nanocarrier: Density functional theory investigation and a molecular dynamics. *Appl. Surf. Sci.* **2017**, *422*, 1030–1041.
[166] Bardajee, G. R.; Hooshyar, Z. Drug release study by a novel thermo sensitive nanogel based on salep modified graphene oxide. *J. Polym. Res.* **2017**, *24*, 49.
[167] Chen, P.; Wang, X.; Wang, G.; Duo, Y. R.; Zhang, X. Y.; Hu, X. H.; Zhang, X. J. Double network self-healing graphene hydrogel by two step method for anticancer drug delivery. *Mater. Technol.* **2014**, *29*, 210–213.
[168] Zhang, H. J.; Zhai, D. D.; He, Y. Graphene oxide/polyacrylamide/carboxymethyl cellulose sodium nanocomposite hydrogel with enhanced mechanical strength: Preparation, characterization and the swelling behavior. *RSC Adv.* **2014**, *4*, 44600–44609.
[169] Kavitha, T.; Kang, I.-K.; Park, S.-Y. Poly(N-vinyl caprolactam) grown on nanographene oxide as an effective nanocargo for drug delivery. *Colloids Surf. B: Biointerfaces* **2014**, *115*, 37–45.
[170] Kundu, A.; Nandi, S.; Das, P.; Nandi, A. K. Fluorescent graphene oxide via polymer grafting: An efficient nanocarrier for both hydrophilic and hydrophobic drugs. *ACS Appl. Mater. Interfaces* **2015**, *7*, 3512–3523.
[171] Pourjavadi, A.; Shakerpoor, A.; Tehrani, Z. M.; Bumajdad, A. Magnetic graphene oxide mesoporous silica hybrid nanoparticles with dendritic pH sensitive moieties coated by PEGylated alginate-*co*-poly (acrylic acid) for targeted and controlled drug delivery purposes. *J. Polym. Res.* **2015**, *22*, 156.
[172] Mahkam, M.; Rafi, A. A.; Faraji, L.; Zakerzadeh, E. Preparation of poly (methacrylic acid)–graphene oxide nanocomposite as a pH-sensitive drug carrier through *in-situ* copolymerization of methacrylic acid with polymerizable graphene. *Polym.-Plast. Technol. Eng.* **2015**, *54*, 916–922.
[173] Zhao, X. B.; Yang, L. W.; Li, X. R.; Jia, X.; Liu, L.; Zeng, J.; Guo, J. S.; Liu, P. Functionalized graphene oxide nanoparticles for cancer cell-specific delivery of antitumor drug. *Bioconjugate Chem.* **2015**, *26*, 128–136.
[174] He, C.; Shi, Z.-Q.; Cheng, C.; Nie, C.-X.; Zhou, M.; Wang, L.-R.; Zhao, C.-S. Highly swellable and biocompatible graphene/heparin-analogue hydrogels for implantable drug and protein delivery. *RSC Adv.* **2016**, *6*, 71893–71904.
[175] Bardajee, G. R.; Hooshyar, Z.; Farsi, M.; Mobini, A.; Sang, G. Synthesis of a novel thermo/pH sensitive nanogel based on salep modified graphene oxide for drug release. *Mater. Sci. Eng. C* **2017**, *72*, 558–565.
[176] Raafat, A. I.; Ali, A. E.-H. pH-controlled drug release of radiation synthesized graphene oxide/(acrylic acid-co-sodium alginate) interpenetrating network. *Polym. Bull.* **2017**, *74*, 2045–2062.
[177] Dai, Z. Q.; Lu, Q. F.; Quan, Q. G.; Mo, R. J.; Zhou, C. X.; Hong, P. Z.; Li, C. Y. Novel low temperature (< 37°C) chitosan hydrogel fabrication under the synergistic effect of graphene oxide. *New J. Chem.* **2017**, *41*, 671–676.
[178] Dragutan, I.; Dragutan, V.; Demonceau, A. Editorial of special issue ruthenium complex: The expanding chemistry of the ruthenium complexes. *Molecules* **2015**, *20*, 17244–17274.
[179] Lee, Y.; Bae, J. W.; Thi, T. T. H.; Park, K. M.; Park, K. D. Injectable and mechanically robust 4-arm PPO–PEO/graphene oxide composite hydrogels for biomedical applications. *Chem. Commun.* **2015**, *51*, 8876–8879.
[180] Yang, H. H.; Bremner, D. H.; Tao, L.; Li, H. Y.; Hu, J.; Zhu, L. M. Carboxymethyl chitosan-mediated synthesis of hyaluronic acid-targeted graphene oxide for cancer drug delivery. *Carbohyd. Polym.* **2016**, *135*, 72–78.

[181] Xu, Z. Y.; Wang, S.; Li, Y. J.; Wang, M. W.; Shi, P.; Huang, X. Y. Covalent functionalization of graphene oxide with biocompatible poly(ethylene glycol) for delivery of paclitaxel. *ACS Appl. Mater. Interfaces* **2014**, *6*, 17268–17276.
[182] Wu, T.; Zhang, B.; Liang, Y. Y.; Liu, T.; Bu, J. Y.; Lin, L. X.; Wu, Z. M.; Liu, H. X.; Wen, S. P.; Tan, S. Z. et al. Heparin-modified graphene oxide loading anti-cancer drug and growth factor with heat stability, long-term release property and lower cytotoxicity. *RSC Adv.* **2015**, *5*, 84334–84342.
[183] Gu, Y. M.; Guo, Y. Z.; Wang, C. Y.; Xu, J. K.; Wu, J. P.; Kirk, T. B.; Ma, D.; Xue, W. A polyamidoamne dendrimer functionalized graphene oxide for DOX and MMP-9 shRNA plasmid co-delivery. *Mater. Sci. Eng. C* **2017**, *70*, 572–585.
[184] Chen, H.; Wang, Z. Y.; Zong, S. F.; Wu, L.; Chen, P.; Zhu, D.; Wang, C. L.; Xu, S. H.; Cui, Y. P. SERS-fluorescence monitored drug release of a redox-responsive nanocarrier based on graphene oxide in tumor cells. *ACS Appl. Mater. Interfaces* **2014**, *6*, 17526–17533.
[185] Khoee, S.; Bafkary, R.; Fayyazi, F. DOX delivery based on chitosan-capped graphene oxide-mesoporous silica nanohybride as pH-responsive nanocarriers. *J. Sol-Gel Sci. Technol.* **2017**, *81*, 493–504.
[186] Wu, H. X.; Shi, H. L.; Wang, Y. P.; Jia, X. Q.; Tang, C. Z.; Zhang, J. M.; Yang, S. P. Hyaluronic acid conjugated graphene oxide for targeted drug delivery. *Carbon* **2014**, *69*, 379–389.
[187] Zhang, B.; Yan, Y. Y.; Shen, Q. J.; Ma, D.; Huang, L. H.; Cai, X.; Tan, S. Z. A colon targeted drug delivery system based on alginate modificated graphene oxide for colorectal liver metastasis. *Mater. Sci. Eng. C* **2017**, *79*, 185–190.
[188] Pan, Q. X.; Lv, Y.; Williams, G. R.; Tao, L.; Yang, H. H.; Li, H. Y.; Zhu, L. M. Lactobionic acid and carboxymethyl chitosan functionalized graphene oxide nanocomposites as targeted anticancer drug delivery systems. *Carbohyd. Polym.* **2016**, *151*, 812–820.
[189] Tan, J. T.; Meng, N.; Fan, Y. T.; Su, Y. T.; Zhang, M.; Xiao, Y. H.; Zhou, N. L. Hydroxypropyl-β-cyclodextrin–graphene oxide conjugates: Carriers for anti-cancer drugs. *Mater. Sci. Eng. C* **2016**, *61*, 681–687.
[190] Lei, H. L.; Xie, M.; Zhao, Y. W.; Zhang, F.; Xu, Y. G.; Xie, J. M. Chitosan/sodium alginate modificated graphene oxide-based nanocomposite as a carrier for drug delivery. *Ceram. Int.* **2016**, *42*, 17798–17805.
[191] Chen, J. Q.; Liu, H. Y.; Zhao, C. B.; Qin, G. Q.; Xi, G. N.; Li, T.; Wang, X. P.; Chen, T. S. One-step reduction and PEGylation of graphene oxide for photothermally controlled drug delivery. *Biomaterials* **2014**, *35*, 4986–4995.
[192] Hou, L.; Shi, Y. Y.; Jiang, G. X.; Liu, W.; Han, H. L.; Feng, Q. H.; Ren, J. X.; Yuan, Y. J.; Wang, Y. C.; Shi, J. J. et al. Smart nanocomposite hydrogels based on azo crosslinked graphene oxide for oral colon-specific drug delivery. *Nanotechnology* **2016**, *27*, 315105.
[193] Liu, J. Q.; Cui, L.; Kong, N.; Barrow, C. J.; Yang, W. R. RAFT controlled synthesis of graphene/polymer hydrogel with enhanced mechanical property for pH-controlled drug release. *Eur. Polym. J.* **2014**, *50*, 9–17.
[194] Byun, E.; Lee, H. Enhanced loading efficiency and sustained release of doxorubicin from hyaluronic acid/graphene oxide composite hydrogels by a mussel-inspired catecholamine. *J. Nanosci. Nanotechnol.* **2014**, *14*, 7395–7401.
[195] Lv, Y.; Tao, L.; Bligh, S. W. A.; Yang, H. H.; Pan, Q. X.; Zhu, L. M. Targeted delivery and controlled release of doxorubicin into cancer cells using a multifunctional graphene oxide. *Mater. Sci. Eng. C* **2016**, *59*, 652–660.
[196] Angelopoulou, A.; Voulgari, E.; Diamanti, E. K.; Gournis, D.; Avgoustakis, K. Graphene oxide stabilized by PLA–PEG copolymers for the controlled delivery of paclitaxel. *Eur. J. Pharm. Biopharm.* **2015**, *93*, 18–26.
[197] Fan, L. H.; Ge, H. Y.; Zou, S. Q.; Xiao, Y.; Wen, H. G.; Li, Y.; Feng, H.; Nie, M. Sodium alginate conjugated graphene oxide as a new carrier for drug delivery system. *Int. J. Biol. Macromol.* **2016**, *93*, 582–590.
[198] Xu, X.; Wang, J.; Wang, Y.; Zhao, L.; Li, Y.; Liu, C. Formation of graphene oxide-hybridized nanogels for combinative anticancer therapy. *Nanomedicine* **2018**, *14*, 2387–2395.
[199] Yu, D. N.; Ruan, P.; Meng, Z. Y.; Zhou, J. P. The structure-dependent electric release and enhanced oxidation of drug in graphene oxide-based nanocarrier loaded with anticancer herbal drug berberine. *J. Pharm. Sci.* **2015**, *104*, 2489–2500.
[200] Guo, Q. F.; Cao, H.; Li, X. H.; Liu, S. W. Thermosensitive hydrogel drug delivery system containing doxorubicin loaded CS–GO nanocarriers for controlled release drug *in situ*. *Mater. Technol.* **2015**, *30*, 294–300.
[201] Pourjavadi, A.; Tehrani, Z. M.; Jokar, S. Chitosan based supramolecular polypseudorotaxane as a pH-responsive polymer and their hybridization with mesoporous silica-coated magnetic graphene oxide for triggered anticancer drug delivery. *Polymer* **2015**, *76*, 52–61.
[202] Mu, S. S.; Li, G. W.; Liang, Y. Y.; Wu, T.; Ma, D. Hyperbranched polyglycerol-modified graphene oxide as an efficient drug carrier with good biocompatibility. *Mater. Sci. Eng. C* **2017**, *78*, 639–646.
[203] Hu, X. H.; Li, D.; Tan, H. P.; Pan, C. B.; Chen, X. X. Injectable graphene oxide/graphene composite supramolecular hydrogel for delivery of anti-cancer drugs. *J. Macromol. Sci. A* **2014**, *51*, 378–384.
[204] Yuan, Y.; Yan, Z. M.; Mu, R. J.; Wang, L.; Gong, J. N.; Hong, X.; Haruna, M. H.; Pang, J. The effects of graphene oxide on the properties and drug delivery of konjac glucomannan hydrogel. *J. Appl. Polym. Sci.* **2017**, *134*, 45327.
[205] Ye, Y. F.; Hu, X. H. A pH-sensitive injectable nanoparticle composite hydrogel for anticancer drug delivery. *J. Nanomater.* **2016**, *2016*, Article ID 9816461.
[206] Saeednia, L.; Yao, L.; Berndt, M.; Cluff, K.; Asmatulu, R. Structural and biological properties of thermosensitive chitosan–graphene hybrid hydrogels for sustained drug delivery applications. *J. Biomed. Mater. Res. A* **2017**, *105*, 2381–2390.
[207] Tian, J. W.; Luo, Y. P.; Huang, L. W.; Feng, Y. Q.; Ju, H. X.; Yu, B.-Y. Pegylated folate and peptide-decorated graphene oxide nanovehicle for *in vivo* targeted delivery of anticancer drugs and therapeutic self-monitoring. *Biosens. Bioelectron.* **2016**, *80*, 519–524.
[208] Huang, Y.-P.; Hung, C.-M.; Hsu, Y.-C.; Zhong, C.-Y.; Wang, W.-R.; Chang, C.-C.; Lee, M.-J. Suppression of breast cancer cell migration by small interfering RNA delivered by polyethylenimine-functionalized graphene oxide. *Nanoscale Res. Lett.* **2016**, *11*, 247.
[209] Masoudipour, E.; Kashanian, S.; Maleki, N. A targeted drug delivery system based on dopamine functionalized nano graphene oxide. *Chem. Phys. Lett.* **2017**, *668*, 56–63.
[210] Alibolandi, M.; Mohammadi, M.; Taghdisi, S. M.; Ramezani, M.; Abnous, K. Fabrication of aptamer decorated dextran coated nano-graphene oxide for targeted drug delivery. *Carbohyd. Polym.* **2017**, *155*, 218–229.
[211] Ma, N. X.; Liu, J.; He, W. X.; Li, Z. H.; Luan, Y. X.; Song, Y. M.; Garg, S. Folic acid-grafted bovine serum albumin decorated graphene oxide: An efficient drug carrier for targeted cancer therapy. *J. Colloid Interface Sci.* **2017**, *490*, 598–607.
[212] Deb, A.; Vimala, R. Natural and synthetic polymer for graphene oxide mediated anticancer drug delivery—A comparative study. *Int. J. Biol. Macromol.* **2018**, *107*, 2320–2333.
[213] Cui, X. J.; Dong, L. L.; Zhong, S. L.; Shi, C.; Sun, Y. X.; Chen, P. Sonochemical fabrication of folic acid functionalized multistimuli-responsive magnetic graphene oxide-based nanocapsules for targeted drug delivery. *Chem. Eng. J.* **2017**, *326*, 839–848.
[214] Shi, Y. F.; Xiong, Z. P.; Lu, X. F.; Yan, X.; Cai, X.; Xue, W. Novel carboxymethyl chitosan-graphene oxide hybrid particles for drug delivery. *J. Mater. Sci.: Mater. Med.* **2016**, *27*, 169.
[215] Wang, J.; Liu, C. H.; Shuai, Y.; Cui, X. Y.; Nie, L. Controlled release of anticancer drug using graphene oxide as a drug-binding effector in konjac glucomannan/sodium alginate hydrogels. *Colloids Surf. B: Biointerfaces* **2014**, *113*, 223–229.
[216] Deng, L.; Li, Q. J.; Al-Rehili, S.; Omar, H.; Almalik, A.; Alshamsan, A.; Zhang, J. F.; Khashab, N. M. Hybrid iron oxide–graphene oxide–polysaccharides microcapsule: A micro-matryoshka for on-demand drug release and antitumor therapy *in vivo*. *ACS Appl. Mater. Interfaces* **2016**, *8*, 6859–6868.
[217] Khatamian, M.; Divband, B.; Farahmand-Zahed, F. Synthesis and characterization of zinc (II)-loaded zeolite/graphene oxide nanocomposite as a new drug carrier. *Mater. Sci. Eng. C* **2016**, *66*, 251–258.
[218] Rasoulzadeh, M.; Namazi, H. Carboxymethyl cellulose/graphene oxide bio-nanocomposite hydrogel beads as anticancer drug carrier agent. *Carbohyd. Polym.* **2017**, *168*, 320–326.
[219] Zhang, H. J.; Yan, T.; Xu, S.; Feng, S. N.; Huang, D. D.; Fujita, M.; Gao, X.-D. Graphene oxide-chitosan nanocomposites for intracellular delivery of immunostimulatory CpG oligodeoxynucleotides. *Mater. Sci. Eng. C* **2017**, *73*, 144–151.
[220] Sudhakar, K.; Moloi, S. J.; Rao, K. M. Graphene oxide/poly(N-isopropyl acrylamide)/sodium alginate-based dual responsive composite beads for controlled release characteristics of chemotherapeutic agent. *Iran. Polym. J.* **2017**, *26*, 521–530.
[221] Wang, R.; Shou, D.; Lv, O. Y.; Kong, Y.; Deng, L. H.; Shen, J. pH-

Controlled drug delivery with hybrid aerogel of chitosan, carboxymethyl cellulose and graphene oxide as the carrier. *Int. J. Biol. Macromol.* **2017**, *103*, 248–253.
[222] Hurt, R. H.; Monthioux, M.; Kane, A. Toxicology of carbon nanomaterials: Status, trends, and perspectives on the special issue. *Carbon* **2006**, *44*, 1028–1033.
[223] Poland, C. A.; Duffin, R.; Kinloch, I.; Maynard, A.; Wallace, W. A. H.; Seaton, A.; Stone, V.; Brown, S.; MacNee, W.; Donaldson, K. Carbon nanotubes introduced into the abdominal cavity of mice show asbestos-like pathogenicity in a pilot study. *Nat. Nanotechnol.* **2008**, *3*, 423–428.
[224] Sanchez, V. C.; Weston, P.; Yan, A. H.; Hurt, R. H.; Kane, A. B. A 3-dimensional *in vitro* model of epithelioid granulomas induced by high aspect ratio nanomaterials. *Part. Fibre Toxicol.* **2011**, *8*, 17.
[225] Li, S. H.; Peng, Z. L.; Han, X.; Leblanc, R. M. Interactions between graphene oxide and biomolecules from surface chemistry and spectroscopy. In *Recent Progress in Colloid and Surface Chemistry with Biological Applications*. American Chemical Society: USA, 2015; pp 43–64.
[226] Jachak, A. C.; Creighton, M.; Qiu, Y.; Kane, A. B.; Hurt, R. H. Biological interactions and safety of graphene materials. *MRS Bull.* **2012**, *37*, 1307–1313.
[227] Hu, C. W.; Liu, L.; Li, X. L.; Xu, Y. D.; Ge, Z. G.; Zhao, Y. J. Effect of graphene oxide on copper stress in *Lemna minor* L.: Evaluating growth, biochemical responses, and nutrient uptake. *J. Hazard. Mater.* **2018**, *341*, 168–176.
[228] Gao, W. The chemistry of graphene oxide. In *Graphene Oxide*. Springer: Switzerland, 2015; pp 61–95.
[229] Li, S. H.; Mulloor, J. J.; Wang, L. Y.; Ji, Y. W.; Mulloor, C. J.; Micic, M.; Orbulescu, J.; Leblanc, R. M. Strong and selective adsorption of lysozyme on graphene oxide. *ACS Appl. Mater. Interfaces* **2014**, *6*, 5704–5712.
[230] Han, S.; Su, L. Q.; Zhai, M. H.; Ma, L.; Liu, S. W.; Teng, Y. A molecularly imprinted composite based on graphene oxide for targeted drug delivery to tumor cells. *J. Mater. Sci.* **2019**, *54*, 3331–3341.
[231] Gurunathan, S.; Kang, M.-H.; Qasim, M.; Kim, J.-H. Nanoparticle-mediated combination therapy: Two-in-one approach for cancer. *Int. J. Mol. Sci.* **2018**, *19*, 3264.
[232] Zamani, M.; Rostami, M.; Aghajanzadeh, M.; Manjili, H. K.; Rostamizadeh, K.; Danafar, H. Mesoporous titanium dioxide@ zinc oxide–graphene oxide nanocarriers for colon-specific drug delivery. *J. Mater. Sci.* **2018**, *53*, 1634–1645.
[233] Vovusha, H.; Sanyal, S.; Sanyal, B. Interaction of nucleobases and aromatic amino acids with graphene oxide and graphene flakes. *J. Phys. Chem. Lett.* **2013**, *4*, 3710–3718.
[234] Liu, B. W.; Salgado, S.; Maheshwari, V.; Liu, J. W. DNA adsorbed on graphene and graphene oxide: Fundamental interactions, desorption and applications. *Curr. Opin. Colloid Interface Sci.* **2016**, *26*, 41–49.
[235] Banerjee, S.; Wilson, J.; Shim, J.; Shankla, M.; Corbin, E. A.; Aksimentiev, A.; Bashir, R. Slowing DNA transport using graphene–DNA interactions. *Adv. Funct. Mater.* **2015**, *25*, 936–946.
[236] Wu, M.; Kempaiah, R.; Huang, P.-J. J.; Maheshwari, V.; Liu, J. W. Adsorption and desorption of DNA on graphene oxide studied by fluorescently labeled oligonucleotides. *Langmuir* **2011**, *27*, 2731–2738.
[237] Becheru, D. F.; Vlăsceanu, G. M.; Banciu, A.; Vasile, E.; Ioniță, M.; Burns, J. S. Optical graphene-based biosensor for nucleic acid detection; influence of graphene functionalization and ionic strength. *Int. J. Mol. Sci.* **2018**, *19*, 3230.
[238] Liu, X. Y.; Sen, S.; Liu, J. Y.; Kulaots, I.; Geohegan, D.; Kane, A.; Puretzky, A. A.; Rouleau, C. M.; More, K. L.; Palmore, G. T. R. et al. Antioxidant deactivation on graphenic nanocarbon surfaces. *Small* **2011**, *7*, 2775–2785.
[239] Shubha, P.; Namratha, K.; Mithali, K.; Divya, V.; Thakur, M. S.; Byrappa, K. Green technology enabled graphene oxide reduction using *Justichia wynaadensis* extract and assessment of *in vitro* antioxidant and antibacterial activity. *Adv. Sci. Lett.* **2018**, *24*, 5726–5730.
[240] Lu, X. L.; Feng, X. D.; Werber, J. R.; Chu, C. C.; Zucker, I.; Kim, J.-H.; Osuji, C. O.; Elimelech, M. Enhanced antibacterial activity through the controlled alignment of graphene oxide nanosheets. *Proc. Natl. Acad. Sci. USA* **2017**, E9793–E9801.
[241] Tang, Z.; Zhao, L.; Yang, Z.; Liu, Z.; Gu, J.; Bai, B.; Liu, J.; Xu, J.; Yang, H. Mechanisms of oxidative stress, apoptosis, and autophagy involved in graphene oxide nanomaterial anti-osteosarcoma effect. *Int. J. Nanomed.* **2018**, *13*, 2907–2919.
[242] Simsikova, M.; Sikola, T. Interaction of graphene oxide with proteins and applications of their conjugates. *J. Nanomed. Res* **2017**, *5*, 00109.
[243] Lee, D. Y.; Khatun, Z.; Lee, J.-H.; Lee, Y.-K.; In, I. Blood compatible graphene/heparin conjugate through noncovalent chemistry. *Biomacromolecules* **2011**, *12*, 336–341.
[244] Hashim, N. C.; Rafie, S. M. M.; Ismail, N. S.; Nordin, D. Effect of the interaction of graphene oxide nanoparticles on a biological model cell membrane. *Eurasian J. Anal. Chem.* **2018**, *13*. DOI: 10.29333/ejac/97221.
[245] Frost, R.; Jönsson, G. E.; Chakarov, D.; Svedhem, S.; Kasemo, B. Graphene oxide and lipid membranes: Interactions and nanocomposite structures. *Nano Lett.* **2012**, *12*, 3356–3362.
[246] Chen, J. L.; Zhou, G. Q.; Chen, L.; Wang, Y.; Wang, X. G.; Zeng, S. W. Interaction of graphene and its oxide with lipid membrane: A molecular dynamics simulation study. *J. Phys. Chem. C* **2016**, *120*, 6225–6231.
[247] Duan, G. X.; Zhang, Y. Z.; Luan, B. Q.; Weber, J. K.; Zhou, R. W.; Yang, Z. X.; Zhao, L.; Xu, J. Y.; Luo, J. D.; Zhou, R. H. Graphene-induced pore formation on cell membranes. *Sci. Rep.* **2017**, *7*, 42767.
[248] Banerjee, A. N. Prospects and challenges of graphene-based nanomaterials in nanomedicine. *Glob. J. Nano.* **2016**, *1*, 555552.
[249] Snitka, V. Graphene based materials: Opportunities and challenges in nanomedicine. *J. Nanomed. Res.* **2015**, *2*, 00035.